Measurement of the production cross-section of a single top quark in association with a W boson at 8 TeV with the ATLAS experiment

The ATLAS collaboration

E-mail: atlas.publications@cern.ch

ABSTRACT: The cross-section for the production of a single top quark in association with a W boson in proton-proton collisions at $\sqrt{s} = 8\,\text{TeV}$ is measured. The dataset corresponds to an integrated luminosity of $20.3\,\text{fb}^{-1}$, collected by the ATLAS detector in 2012 at the Large Hadron Collider at CERN. Events containing two leptons and one central b-jet are selected. The Wt signal is separated from the backgrounds using boosted decision trees, each of which combines a number of discriminating variables into one classifier. Production of Wt events is observed with a significance of 7.7σ. The cross-section is extracted in a profile likelihood fit to the classifier output distributions. The Wt cross-section, inclusive of decay modes, is measured to be $23.0\pm1.3(\text{stat.})^{+3.2}_{-3.5}(\text{syst.})\pm1.1(\text{lumi.})$ pb. The measured cross-section is used to extract a value for the CKM matrix element $|V_{tb}|$ of 1.01 ± 0.10 and a lower limit of 0.80 at the 95% confidence level. The cross-section for the production of a top quark and a W boson is also measured in a fiducial acceptance requiring two leptons with $p_{\text{T}} > 25\,\text{GeV}$ and $|\eta| < 2.5$, one jet with $p_{\text{T}} > 20\,\text{GeV}$ and $|\eta| < 2.5$, and $E_{\text{T}}^{\text{miss}} > 20\,\text{GeV}$, including both Wt and top-quark pair events as signal. The measured value of the fiducial cross-section is $0.85 \pm 0.01(\text{stat.})^{+0.06}_{-0.07}(\text{syst.})\pm0.03(\text{lumi.})$ pb.

doi:10.1007/JHEP01(2016)064

Contents

1 Introduction

The production of a single top quark at the Large Hadron Collider (LHC) proceeds via the weak interaction in the Standard Model (SM). The three main modes of single top-quark production are: t-channel, the exchange of a W boson between a light quark and a heavy quark; s-channel, via a virtual W boson; and Wt, the production of a top quark in association with a W boson. Single top-quark production depends on the top-quark coupling to the W boson, which is parameterised by the form factor $f_{\rm LV}$ and the Cabibbo-Kobayashi-Maskawa (CKM) matrix element V_{tb} [1–3]. The cross-section for each of the three production modes is proportional to the square of $|f_{\rm LV}V_{tb}|$ [4, 5]. Physics beyond the SM can contribute to the single top-quark final state and modify the production cross-sections [6, 7] as well as the kinematic distributions, for example through a resonance that decays to Wt [8, 9].
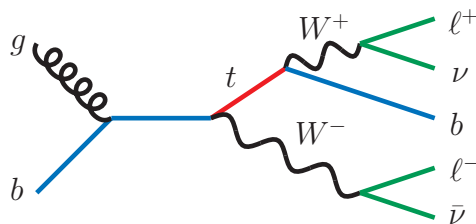
– 1 –

Figure 1. Representative leading-order Feynman diagram for the production and decay of a single top quark in association with a W boson.

The production of single top quarks has been observed at the Tevatron proton-antiproton collider in the t-channel [10, 11] and s-channel [12–14], as well as their combination [15–17]. The Wt process has a small expected cross-section at the Tevatron and was not observed. The t-channel mode has been observed by both the ATLAS [18, 19] and CMS [20, 21] collaborations at the LHC. The s-channel mode has not yet been measured at the LHC because of its small production cross-section [22]. Evidence for Wt production was reported by ATLAS [23] and CMS [24] in proton-proton (pp) collisions at 7 TeV. The observation of Wt production in pp collisions at 8 TeV has been reported by CMS [25].

Production of Wt events proceeds via b-quark-induced partonic channels such as $gb \rightarrow Wt \rightarrow W^-W^+b$. A leading-order (LO) Feynman diagram in the 5-flavour-number scheme (5FNS, considering the quarks u, d, s, c, and b in the initial state) is shown in figure 1. The presence of only a single b-quark in the final state represents a distinctive feature with respect to the $W^+W^-b\bar{b}$ final state of top-quark pair ($t\bar{t}$) production. The Wt final state contains an additional b-quark in higher-order Quantum Chromodynamics (QCD) correction diagrams in the 5FNS, as well as in the leading-order process in the 4-flavour-number scheme (4FNS, considering only the quarks u, d, s, c in the initial state), making it challenging to experimentally separate Wt production from $t\bar{t}$ production.

The theoretical prediction for the Wt production cross-section at next-to-leading order (NLO) with next-to-next-to-leading logarithmic (NNLL) soft gluon corrections is 22.37 ± 1.52 pb [26] at a centre-of-mass energy of $\sqrt{s} = 8$ TeV for a top-quark mass of $m_t = 172.5$ GeV [27]. In this calculation, the uncertainty on the theoretical cross-section accounts for the variation of the renormalisation and factorisation scale between $m_t/2$ and $2m_t$ and for the parton distribution function (PDF) uncertainties (using the 90% confidence level errors of the MSTW2008 NNLO PDF set [28]). This cross-section represents about 20% of the total cross-section for all single top-quark production modes at the LHC. A second theoretical prediction for the Wt production cross-section is 18.8 ± 0.8 (scale) ± 1.7 (PDF) pb, computed at NLO with Hathor v2.1 [29, 30]. The PDF uncertainties are calculated using the PDF4LHC prescription [31] with three different PDF sets (CT10, MSTW2008NLO68CL [28] and NNPDF2.3 [32]). The renormalisation and factorisation scales are set to 65 GeV and the b-quark from initial-state radiation is required to have a transverse momentum of less than 60 GeV.

This paper presents a measurement of the cross-section for Wt production in pp collisions at $\sqrt{s} = 8$ TeV, based on the analysis of $20.3\,\mathrm{fb}^{-1}$ of data collected by the ATLAS

detector in 2012. The measurement is carried out in the dilepton final state shown in figure 1 where each W boson decays to an electron or a muon and a neutrino ($e\nu$ or $\mu\nu$). This analysis requires two opposite-sign high-transverse-momentum (p_T) leptons (ee, $e\mu$, $\mu\mu$), missing transverse momentum (E_T^{miss}), and one high-p_T central jet, which is required to contain a b-hadron (b-jet). The main background to this signature is from $t\bar{t}$ production, with smaller backgrounds coming from dibosons (WW, WZ, ZZ), Z+jets, and events where one or both leptons are misidentified (fake-lepton events) or non-prompt. Control regions enriched in $t\bar{t}$ and other background events are also defined. Events in the $t\bar{t}$-enriched regions fulfil the same lepton and missing transverse momentum requirements, and have exactly two jets, with one or both of the jets required to be identified as a b-jet. Events in the other background-enriched regions have one or two jets which are required to not be identified as b-jets. The backgrounds are estimated with simulation, except the non-prompt or fake-lepton background, which is estimated from data. Boosted decision trees (BDT) are used to optimise the discrimination between signal and background [33]. The cross-section is extracted using a profile likelihood fit of the BDT response. The background normalisation and the systematic uncertainties are constrained by simultaneously analysing phase-space regions with substantial Wt signal contributions and regions where the Wt contributions are negligible. The ratio of the measured cross-section to the theoretical prediction (which assumes $V_{tb} = 1$) is used to extract a value of $|f_{LV}V_{tb}|$.

In the 5FNS, the Wt single top-quark process overlaps and interferes with $t\bar{t}$ production at NLO where diagrams involving two top quarks are part of the real emission corrections to Wt production [34, 35]. A calculation in the 4FNS scheme includes Wt and $t\bar{t}$ as well as non-top-quark diagrams [36] and the interference between Wt and $t\bar{t}$ enters already at tree level. A measurement of the cross-section inside a fiducial acceptance, designed to reduce the dependence on the theory assumptions, is also presented. The fiducial acceptance is defined using physics objects constructed of stable particles to approximate the Wt detector acceptance. The cross-section for the sum of Wt and $t\bar{t}$ production is measured in this fiducial acceptance.

This paper is organised as follows: section 2 provides a brief overview of the ATLAS detector and the definition of physics objects. Section 3 describes the data and Monte Carlo samples used for the analysis. Section 4 describes the event selection and background estimation. Section 5 presents the procedure defined to discriminate the signal from the backgrounds using BDTs. The dominant systematic uncertainties are discussed in section 6. Section 7 presents the results for the inclusive cross-section measurement and for $|V_{tb}|$ and discusses the impact of systematic uncertainties. Section 8 defines the fiducial acceptance and presents the fiducial cross-section measurement. Finally, a summary is presented in section 9.

2   The ATLAS detector and object reconstruction

The ATLAS detector [37] is a multi-purpose particle detector with a forward-backward symmetric cylindrical geometry and a near 4π coverage in solid angle.[1] ATLAS comprises

---

[1]ATLAS uses a right-handed coordinate system with its origin at the nominal interaction point (IP) in the centre of the detector and the z-axis along the beam pipe. The x-axis points from the IP to the centre

an inner detector (ID) surrounded by a thin superconducting solenoid providing a 2 T axial magnetic field, a calorimeter system and a muon spectrometer in a toroidal magnetic field. The ID tracking system covers the pseudorapidity range $|\eta| < 2.5$ and consists of silicon pixel, silicon microstrip, and transition radiation tracking detectors. The ID provides precise position and momentum measurements for charged particles and allows efficient identification of jets containing b-hadrons. Lead/liquid-argon (LAr) sampling calorimeters provide electromagnetic (EM) energy measurements with high granularity up to $|\eta| = 2.5$. A hadron (steel/scintillator-tile) calorimeter covers the central pseudorapidity range ($|\eta| < 1.7$). The end-cap and forward regions are instrumented with LAr calorimeters for both the EM and hadronic energy measurements up to $|\eta| = 4.9$. The muon spectrometer surrounds the calorimeters. It consists of three large air-core toroid superconducting magnet systems, separate trigger detectors and high-precision tracking chambers providing accurate muon tracking for $|\eta| < 2.7$ and muon triggering for $|\eta| < 2.4$.

A three-level trigger system [38] is used to select events. The first-level trigger is implemented in hardware and uses a subset of the detector information to reduce the event rate to less than 75 kHz. Two software-based trigger levels, Level-2 and the Event Filter, reduce the rate of Level-1 accepts to about 400 Hz on average.

Candidate events are characterised by exactly two leptons (ee, $\mu\mu$, $e\mu$), missing transverse momentum $E_{\mathrm{T}}^{\mathrm{miss}}$ due to the neutrinos from the leptonic decays of the two W bosons, and a b-jet originating from the top-quark decay. Electron candidates are reconstructed from energy clusters in the calorimeter which are matched to ID tracks [39]. Selected electrons must have $E_{\mathrm{T}} > 25$ GeV and $|\eta| < 2.47$, excluding the barrel/end-cap transition region of $1.37 < |\eta| < 1.52$. A hit in the innermost layer of the ID is required, to reject photon conversions. Electron candidates are required to fulfil calorimeter-based and track-based isolation requirements in order to suppress backgrounds from hadron decays. The calorimeter transverse energy within a cone of size $\Delta R = 0.2$ and the scalar sum of track p_{T} within ΔR of 0.3 around the electron, in each case excluding the contribution from the electron itself, are each required to be smaller than E_{T}- and η-dependent thresholds calibrated to give nominal selection efficiencies of 90% for prompt electrons from $Z \to ee$ decays.

Muon candidates are reconstructed by combining matching tracks reconstructed in both the ID and the muon spectrometer [40]. Selected muons have a $p_{\mathrm{T}} > 25$ GeV and $|\eta| < 2.5$. An isolation criterion [41] is applied in order to reduce background contamination from events in which a muon candidate is accompanied by hadrons. The ratio of the sum of p_{T} of additional tracks in a variable-size cone around the muon, to the p_{T} of the muon [41], is required to be less than 0.05, yielding a selection efficiency of 97% for prompt muons from $Z \to \mu\mu$ decays.

Jets are reconstructed using the anti-k_t jet clustering algorithm [42] with a radius parameter of $R = 0.4$, using locally calibrated topological clusters as inputs [43]. Jet energies are calibrated using energy- and η-dependent correction factors derived from simulation and with residual corrections from in-situ measurements [44]. Jets are required to be re-

---

of the LHC ring, and the y-axis points upwards. Cylindrical coordinates (r, ϕ) are used in the transverse plane, ϕ being the azimuthal angle around the z-axis. The pseudorapidity is defined in terms of the polar angle θ as $\eta = -\ln\tan(\theta/2)$. Angular separation is measured in units of $\Delta R \equiv \sqrt{(\Delta\eta)^2 + (\Delta\phi)^2}$.

constructed in the range $|\eta| < 2.5$ and to have $p_\mathrm{T} > 20$ GeV. To reduce the contamination due to jets from additional pp interactions in the same or neighbouring bunch crossings (pileup), tracks originating from the primary vertex must contribute a large fraction to the scalar sum of the p_T of all tracks in the jet. This jet vertex fraction (JVF) [45] is required to be at least 50% for jets with $p_\mathrm{T} < 50$ GeV and $|\eta| < 2.4$.

To avoid double-counting objects in an event and to suppress leptons from heavy-flavour decays, overlaps between reconstructed objects are resolved in the following order: (1) jets overlapping with a selected electron within ΔR of 0.2 are removed; (2) electrons that are within ΔR of 0.4 of a jet are removed; (3) events are rejected if a selected electron shares an ID track with a selected muon; and (4) muons that are within ΔR of 0.4 of a jet are removed.

The identification of b-jets relies of the long lifetime of b-hadrons and the topological properties of secondary and tertiary decay vertices reconstructed within the jet. A combination of multivariate algorithms is used to identify b-jets (b-tag) [46]. The b-tag algorithm has an average efficiency of 70% for b-jets from $t\bar{t}$ decays and an average mis-tag rate of 0.8% [47, 48] for light-quark jets.

The missing transverse momentum ($E_\mathrm{T}^\mathrm{miss}$) is calculated as the magnitude of the vector sum over the energies of all clusters in the calorimeters, and is refined by applying object-level corrections to the contributions arising from identified electrons, muons, and jets [49].

3 Data and simulated samples

The dataset used for this analysis was collected at $\sqrt{s} = 8$ TeVin 2012 by the ATLAS detector at the LHC, and corresponds, after data quality requirements, to an integrated luminosity of $20.3\,\mathrm{fb}^{-1}$. Events are required to have fired either a single-electron or single-muon trigger. The electron and muon triggers impose a p_T threshold of 24 GeV, along with isolation requirements on the lepton. To recover efficiency for higher p_T leptons, the isolated lepton triggers are complemented by triggers without isolation requirements, but with p_T thresholds of 60 GeV and 36 GeV for electrons and muons respectively.

Samples of signal and background events are simulated using various Monte Carlo (MC) generators, as summarised in table 1. The generators used for the estimation of the modelling uncertainties are listed together with the reference simulation for the Wt signal and the $t\bar{t}$ background. In addition, PDFs used by each generator and the perturbative order in QCD of the respective calculations are provided. All simulation samples are normalised to theoretical cross-section predictions. A top-quark mass of 172.5 GeV is used [27].

The Wt events are simulated using the NLO generator POWHEG-BOX [50, 51], interfaced to PYTHIA [52] for parton showering with the Perugia 2011C set of tuned parameters [53]. In the POWHEG-BOX event generator, the CT10 [54] PDFs are used, while the CTEQ6L1 [55] PDFs are used for PYTHIA. The generation of Wt events is performed in the 5FNS. The overlap and interference between Wt and $t\bar{t}$ is handled using the diagram-removal scheme (DR), where all doubly resonant NLO Wt diagrams are removed [56]. An additional sample, generated with the diagram-subtraction scheme (DS), where the cross-

Process	Generator	PDF	Normalisation
Wt	Powheg-Box v1.0	CT10	
	+ Pythia v6.426, DR	CTEQ6L1	
Wt †	Powheg-Box v1.0	CT10	
	+ Pythia v6.426, DS	CTEQ6L1	22.37 pb
Wt †	Powheg-Box v1.0	CT10	(NLO+NNLL)
	+ Herwig v6.520.2, DR	CT10	
Wt †	MC@NLO v4.06	CT10	
	+ Herwig v6.520.2, DR	CT10	
$t\bar{t}$	Powheg-Box v1.0	CT10	
	+ Pythia v6.426	CTEQ6L1	
$t\bar{t}$ †	Powheg-Box v1.0	CT10	253 pb
	+ Herwig v6.520.2	CT10	(NNLO+NNLL)
$t\bar{t}$ †	MC@NLO v4.06	CT10	
	+ Herwig v6.520.2	CT10	
WW, WZ, ZZ	Alpgen v2.1.4	CTEQ6L1	88 pb
	+ Herwig v6.520.2	CT10	(NLO)
$Z(\to ee, \mu\mu, \tau\tau)$ + jets	Alpgen v2.1.4	CTEQ6L1	3450 pb
	+ Pythia v6.426	CTEQ6L1	(NNLO)

Table 1. Monte Carlo generators used to model the Wt signal and the background processes at $\sqrt{s} = 8$ TeV. The samples marked with a † are used as alternatives for Wt or $t\bar{t}$ to evaluate modelling uncertainties. DR refers to the diagram-removal scheme and DS to the diagram-subtraction scheme to handle the overlap and interference between Wt and $t\bar{t}$, as discussed in the text.

section contribution from Feynman diagrams containing two top quarks is subtracted, is used to evaluate the uncertainty associated with the modelling of the overlap between Wt and $t\bar{t}$ [56]. Two alternative samples are used to determine theory modelling uncertainties: one using MC@NLO [57] and the other using Powheg-Box, both interfaced to Herwig [58], with Jimmy for underlying-event modelling [59].

The dominant and largely irreducible $t\bar{t}$ background is simulated with Powheg-Box, using the CT10 NLO PDF set, with parton showering and hadronisation performed with Pythia. The $t\bar{t}$ production cross-section is $\sigma_{t\bar{t}} = 253^{+13}_{-15}$ pb, computed at NNLO in QCD, including resummation of NNLL soft gluon terms [60–66].

Smaller backgrounds arise from diboson and Z+jets production. The Alpgen LO generator [67], interfaced to Herwig, is used to generate diboson events, with the CTEQ6L1 PDF set. Diboson events are normalised to the NLO prediction [68]. The Z+jets background is generated with Alpgen, interfaced to Pythia, with the CTEQ6L1 PDF set. The diboson estimate also accounts for lower cross-section diboson processes, including $H \to WW$. The Z+jets events are normalised to the NNLO prediction [69].

The non-prompt or fake-lepton background arises from non-prompt electrons or muons from the weak decay of mesons events, or from events where one or both leptons are mis-identified. This background contribution includes the t-channel and s-channel single top-quark production modes. The normalisation and shape of the non-prompt or fake-lepton background is determined directly from data, using the matrix method [70]. In addition to events from the signal data sample (labelled as "tight" events), a second ("loose") set enriched with fake leptons is defined by removing the lepton isolation requirement. Given the probabilities for real and fake leptons that already passed the loose selection to also pass the tight selection, the number of tight events with a fake lepton is determined from a linear system of equations.

Generated events are passed through a simulation [71] of the ATLAS detector based on GEANT4 [72] and reconstructed using the same procedure as for collision data. The alternative $t\bar{t}$ samples used to evaluate theory modelling uncertainties are instead processed with the ATLFAST-II [71] simulation, which employs a parameterisation of the response of the electromagnetic and hadronic calorimeters, and GEANT4 for the other detector components. The simulations also include the effect of multiple pp collisions per bunch crossing (pileup).

4   Event selection

The dilepton selection requires that each event has a high-quality reconstructed primary vertex, which must be formed from at least five tracks with $p_T > 0.4$ GeV. Each selected event must contain exactly two isolated opposite-sign leptons (e, μ) that originate from the primary vertex, at least one of which must be associated with a lepton that triggered the event. In addition, since the Wt signature contains a high-p_T quark from the top-quark decay, events are required to have either one jet or two jets.

Events from Z-boson decays (including $Z \to ee$, $Z \to \mu\mu$, and $Z \to \tau\tau$ with $\tau \to e$ or μ) are suppressed through requirements on the invariant mass of the dilepton system as well as on E_T^{miss} and the pseudorapidity of the leptons+jet(s) system. Events containing same-flavour leptons (ee or $\mu\mu$) are rejected if the invariant mass of the lepton pair is between 81 GeV and 101 GeV. Events are also required to have $E_T^{\mathrm{miss}} > 40$ GeV, with the threshold raised to 70 GeV if the invariant mass of the lepton pair is below 120 GeV. Events containing one electron and one muon are required to have $E_T^{\mathrm{miss}} > 20$ GeV, with the threshold raised to 50 GeV if the invariant mass of the lepton pair is below 80 GeV. Since Wt events are more central than Z+jets events, the pseudorapidity of the system of both leptons and all jets, reconstructed from the vectorial sum of lepton and jet momenta, is required to be $|\eta^{\mathrm{sys}}| < 2.5$.

Events are categorised into five regions depending on the jet and b-tag multiplicities. The largest number of expected signal events is in the 1-jet region with one b-tagged jet, while events in the two-jet regions with one or two b-tags are dominated by $t\bar{t}$. These three regions are included in the cross-section fit. Two additional regions are used to validate the modelling of the other backgrounds but are not included in the fit. One-jet and two-jet events that have zero b-tagged jets compose the 0-tag control regions, which are enhanced

Process	1-jet 1-tag	2-jet 1-tag	2-jet 2-tag	1-jet 0-tag	2-jet 0-tag
Wt	1000(140)	610(70)	160(50)	660(100)	290(30)
$t\bar{t}$	4500(700)	7600(900)	5000(900)	2600(400)	2660(330)
Diboson	40(30)	35(15)	1(1)	1600(500)	670(270)
Z + jets	70(40)	60(40)	7(4)	2600(1400)	900(500)
Non-prompt or fake lepton	24(15)	27(15)	13(7)	130(70)	80(50)
Total background	4600(700)	7700(900)	5000(900)	6900(1400)	4300(600)
Signal+Background	5600(800)	8300(900)	5200(900)	7600(1500)	4600(600)
Observed	5585	8371	5273	7530	4475

Table 2. Numbers of expected events for the Wt signal and the various background processes and observed events in data in the five regions, with their predicted uncertainties. Uncertainties shown include all sources of statistical and systematic uncertainty, summed in quadrature.

in the other backgrounds. Observed yields and kinematic distributions in the 0-tag control regions are studied while choosing the selection cuts; the three regions included in the cross-section fit are not part of this optimisation procedure.

The predicted event yields for signal and backgrounds, and their uncertainties, are summarised in table 2. Uncertainties from different sources are added in quadrature, not taking into account possible correlations. Many of the sources of systematic uncertainty are common to the Wt signal and $t\bar{t}$ background processes, and correlated between regions (see section 6). The numbers of events observed in data and the total predicted yields are compatible within the uncertainties. The Wt signal comprises 21% of the total expected event yield in the 1-jet 1-tag region. The main background originates from the production of top-quark pair events, which accounts for almost 80% of the total event yield in the 1-jet 1-tag region. For the other regions included in the fit, the expected fraction of signal events is smaller, 9% in the 2-jet 1-tag region and 3% in the 2-jet 2-tag region, which is the most enriched in $t\bar{t}$. The other backgrounds are small in the 1-jet 1-tag and 2-jet regions where they account for 2% of the total event yield. The 0-tag control regions are enriched in other backgrounds (diboson, Z+jets and non-prompt or fake lepton), which contribute 40–60% of the total event yield.

The $E_{\mathrm{T}}^{\mathrm{miss}}$ distributions of events in the 0-tag regions are shown in figure 2 to demonstrate the good modelling of the other backgrounds. The behaviour of this distribution at low $E_{\mathrm{T}}^{\mathrm{miss}}$ values is a result of the different requirements for same-flavour and opposite-flavour leptons. Figures 3 and 4 show the distributions of kinematic variables of reconstructed objects for the three b-tagged regions. The data distributions are well modelled by the background and signal expectations in all regions.

5   Analysis

The separation of the Wt signal from the dominant background from top-quark pairs is accomplished through the use of a BDT algorithm [33] in the TMVA framework [73]. The BDTs are trained separately in three regions, 1-jet 1-tag, 2-jet 1-tag and 2-jet 2-tag, using simulated Wt events as signal and simulated $t\bar{t}$ events as background. Three
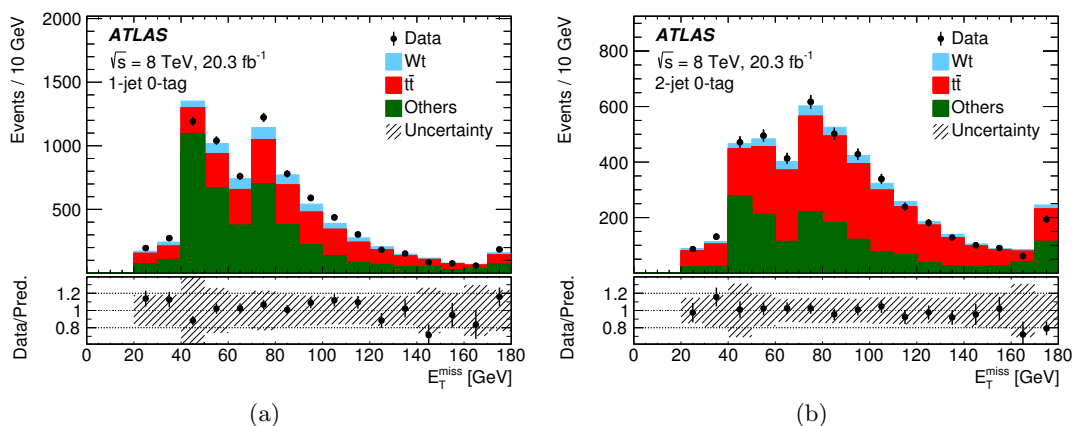
Figure 2. Distributions of the missing transverse momentum E_T^{miss} in (a) 1-jet and (b) 2-jet events with 0 b-tags. The simulated signal and background contributions are scaled to their expectations. The hatched area represents the sum in quadrature of the statistical and systematic uncertainties. The last bin includes the overflow.

Figure 3. Distributions, in the 1-jet 1-tag region, of (a) p_T of the leading lepton (ℓ_1), (b) p_T of the second-leading lepton (ℓ_2), (c) p_T of the jet (j_1), and (d) E_T^{miss}. The simulated signal and background contributions are scaled to their expectations. The hatched area represents the sum in quadrature of the statistical and systematic uncertainties. The last bin includes the overflow.
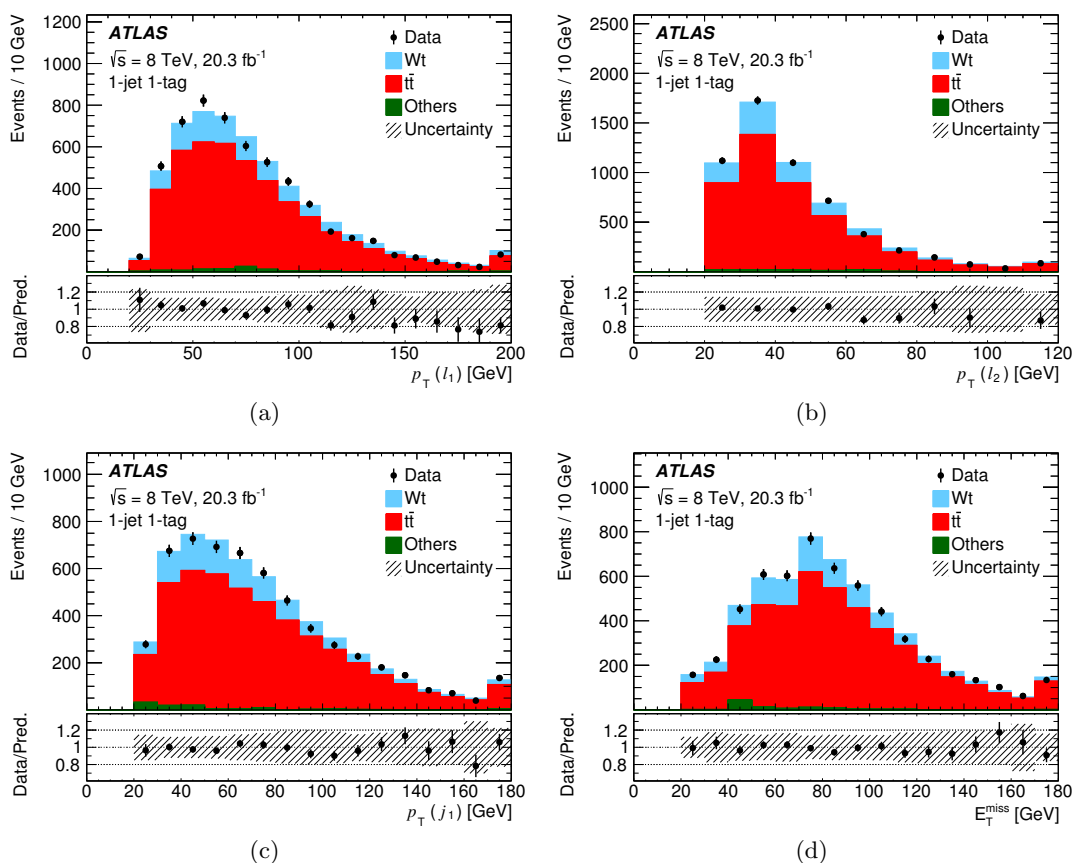
Figure 4. Distributions of the p_T of the leading jet (j_1) and the second-leading jet (j_2) in the (a,b) 2-jet 1-tag and (c,d) 2-jet 2-tag regions. The simulated signal and background contributions are scaled to their expectations. The hatched area represents the sum in quadrature of the statistical and systematic uncertainties. The last bin includes the overflow.
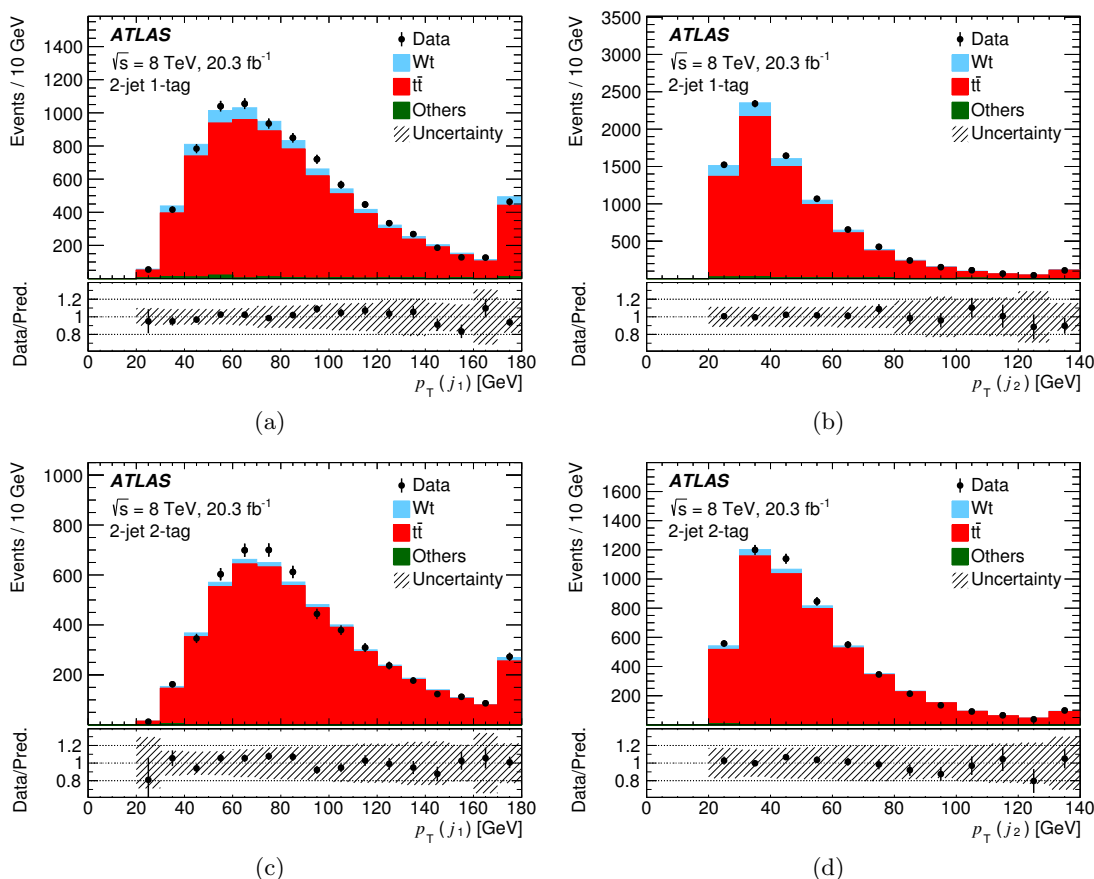
equal-size Wt samples are combined to reduce sensitivity to the modelling uncertainties and to maximise the number of events available for training: the POWHEG-BOX+PYTHIA sample with the DR scheme, the POWHEG-BOX+PYTHIA sample with the DS scheme, and the POWHEG-BOX+HERWIG sample with the DR scheme. The ADABOOST boosting algorithm is used [74]. This algorithm increases the event weight for mis-classified events for consecutive trees in the training. The final BDT is then the weighted average over all trees. The list of variables entering the BDT algorithm is chosen based on the power to discriminate the Wt signal from the $t\bar{t}$ background and is derived from a large set of kinematic variables that show good agreement between data and MC simulation. The number of input variables is a compromise between the achievable discrimination power and possible overtraining. As a result of this optimisation procedure, 13, 16, and 16 variables are selected for the 1-jet 1-tag, 2-jet 1-tag, and 2-jet 2-tag regions, respectively.

The BDT input variables used in the three regions are explained below and are listed in table 3 together with their importance ranking. The objects (denoted $o_1, \ldots, o_n$) used to define these kinematic variables are the leading- and second-leading lepton (ℓ_1 and ℓ_2) and jet (j_1 and j_2) as well as E_T^{miss}. The kinematic variables are defined as follows.

- $p_{\mathrm{T}}^{\mathrm{sys}}(o_1, \ldots, o_n)$, magnitude of the vector sum of the transverse momenta of the objects.

- $\sum E_{\mathrm{T}}$, the scalar sum of transverse energy of calorimeter cells. For cells associated with electrons and jets, the corresponding corrections are applied.

- $\sigma\ (p_{\mathrm{T}}^{\mathrm{sys}}(o_1, \ldots, o_n))$, the ratio of $p_{\mathrm{T}}^{\mathrm{sys}}$ to $(H_{\mathrm{T}} + \sum E_{\mathrm{T}})$, where H_{T} is the scalar sum of the transverse momenta of the objects.

- $\Delta p_{\mathrm{T}}(o_1, o_2)$, the difference in p_{T} between the two objects.

- $\Delta R(o_1, o_2)$, the separation of the two objects in ϕ–η space.

- $m_{\mathrm{T}}(o_1, o_2)$, the transverse mass, given by $\sqrt{2p_{\mathrm{T}}(o_1)p_{\mathrm{T}}(o_2)(1 - \cos \Delta\phi)}$.

- Centrality(o_1, o_2), the ratio of the scalar sum of the p_{T} of the two objects to the sum of their energies.

- $m(o_1, o_2)$, the invariant mass of the system of the two objects.

- $m_{\mathrm{T}2}$, which contains information about the presence of the two neutrinos from the two W-boson decays [75–77]. The $m_{\mathrm{T}2}$ algorithm creates candidates for the transverse momenta of the two neutrinos, which must sum to give the missing transverse momentum. These are combined with the momenta of the two leptons to form the transverse mass of two candidate W bosons, with each also fulfilling a W-boson mass constraint. For each such candidate pair, the larger of the two transverse masses is kept. Then $m_{\mathrm{T}2}$ is given by the smallest transverse mass in all possible candidate pairs.

- $E/m(o_1, o_2, o_3)$, the ratio of the energy of the system of the three objects to the invariant mass of this system.

Figure 5 compares the shapes of the most important variables in the 1-jet 1-tag region for Wt and $t\bar{t}$ events and shows a comparison of the data and the SM predictions. The most important variable is $p_{\mathrm{T}}^{\mathrm{sys}}(\ell_1, \ell_2, E_{\mathrm{T}}^{\mathrm{miss}}, j_1)$, which is sensitive to the unidentified b-quark in $t\bar{t}$ events. This variable peaks at lower values for Wt and has a longer tail for $t\bar{t}$. The second most important variable is the separation of the leading lepton and the jet, in ϕ-η space. These two objects originate from the same top quark in Wt events, leading to a sharper peak than in $t\bar{t}$ events. Figure 6 shows the most important discriminating variables in the 2-jet regions. Here, the $p_{\mathrm{T}}^{\mathrm{sys}}$ distribution also peaks at lower values for Wt than for $t\bar{t}$, but the distribution is also broader for Wt, resulting in a long tail. The invariant mass variables are important for 2-jet events, where half of the possible lepton-jet pairings correspond to the objects from the decay of one of the top quarks in $t\bar{t}$ events leading to a peak at lower invariant mass. For Wt, only one quarter of the possible pairings of jets and leptons correspond to the objects from the top-quark decay.

The BDT response for the three regions is shown in figure 7. The Wt signal is larger at positive BDT response values, while the $t\bar{t}$ background dominates for negative BDT

Variable	1-jet, 1-tag	2-jet 1-tag	2-jet 2-tag
$p_T^{sys} (\ell_1, \ell_2, E_T^{miss}, j_1)$	1		
$p_T^{sys} (\ell_1, \ell_2, j_1)$	7		
$p_T^{sys} (\ell_1, \ell_2)$	13		
$p_T^{sys} (j_1, j_2)$		10	1
$p_T^{sys} (\ell_1, \ell_2, E_T^{miss})$		12	2
$p_T^{sys} (\ell_1, \ell_2, E_T^{miss}, j_1, j_2)$		13	
$p_T^{sys} (\ell_1, j_1)$			13
$\sigma(p_T^{sys}) (\ell_1, \ell_2, E_T^{miss}, j_1)$	4	5	
$p_T (j_2)$			8
$\Delta p_T (\ell_1, \ell_2)$	8		
$\Delta p_T ((\ell_1, \ell_2, j_1), (E_T^{miss}))$	9		
$\Delta p_T (E_T^{miss}, j_1)$		9	
$\Delta p_T (\ell_1, \ell_2, E_T^{miss}, j_1)$		16	
$\Delta p_T (\ell_2, j_2)$			14
$\Delta R (\ell_1, j_1)$	2		5
$\Delta R (\ell_2, j_1)$		4	10
$\Delta R (\ell_2, j_2)$		6	
$\Delta R (\ell_2, j_1)$		11	
$\Delta R (\ell_1, \ell_2)$		14	
$\Delta R ((\ell_1, \ell_2), j_2)$			9
$m (\ell_2, j_1)$	10	3	3
$m (\ell_1, j_2)$		1	4
$m (j_1, j_2)$		2	
$m (\ell_2, j_2)$		7	7
$m (\ell_1, j_1)$		8	6
$m (\ell_1, \ell_2)$		15	
$m (\ell_2, j_1, j_2)$			11
$m (\ell_1, \ell_2, j_1, j_2)$			15
$m_T (j_1, E_T^{miss})$	5		
m_{T2}	11		
$E/m (\ell_1, \ell_2, j_2)$			16
$\sum E_T$	3		
Centrality(ℓ_1, ℓ_2)	6		
Centrality(ℓ_1, j_1)	12		
Centrality(ℓ_2, j_2)			12

Table 3. Discriminating variables used in the training of the BDT for each region. The number indicates the relative importance of this variable, with 1 referring to the most important variable. An empty field means that this variable is not used in this region.
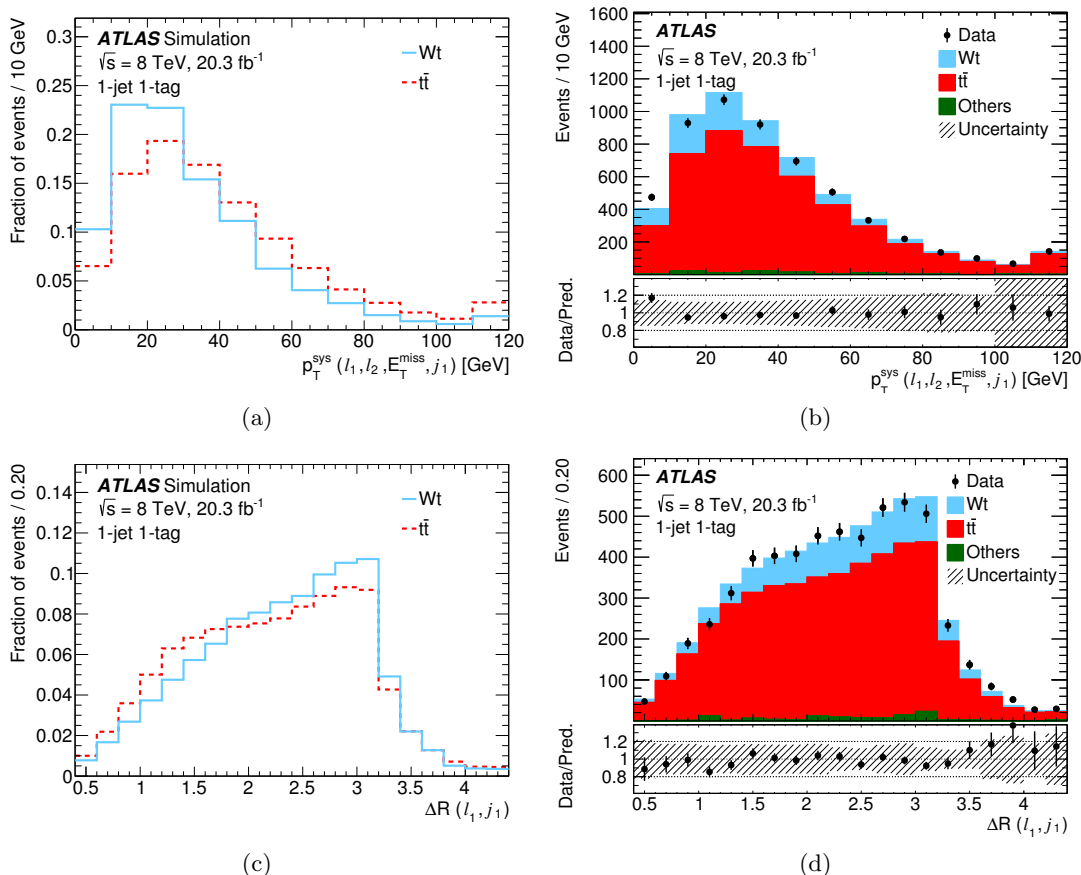
Figure 5. Distributions of the two most important BDT input variables for the 1-jet 1-tag region. The distributions are shown for (a, b) the p_T of the system of the leptons, jet and E_T^{miss} and (c, d) the ΔR between the leading lepton and the jet. Each contribution is normalised to unit area in (a, c) and to its expectation in (b, d). The hatched area represents the sum in quadrature of the statistical and systematic uncertainties. The last bin includes the overflow.

response values. The BDT range in each region is chosen to ensure sufficient simulation statistics in each bin. The BDT separates the signal from the background in all three regions, although even for high BDT response values in the 1-jet 1-tag region, there remains a large expected background from $t\bar{t}$ events. The BDT responses from figure 7 are used in the profile likelihood fit swith this binning.

6 Systematic uncertainties

Systematic uncertainties affect the acceptance estimates for the signal and background processes. Some of the systematic uncertainties also affect the shape of the BDT response. Experimental sources of uncertainty arise from the modelling of jets, leptons and E_T^{miss}.

The impact of the uncertainty in the jet energy scale (JES) on the acceptance and shape of the BDT response for Wt and $t\bar{t}$ is evaluated in 22 uncorrelated components, each of which can have a p_T and η dependence [44, 78]. The largest components are related
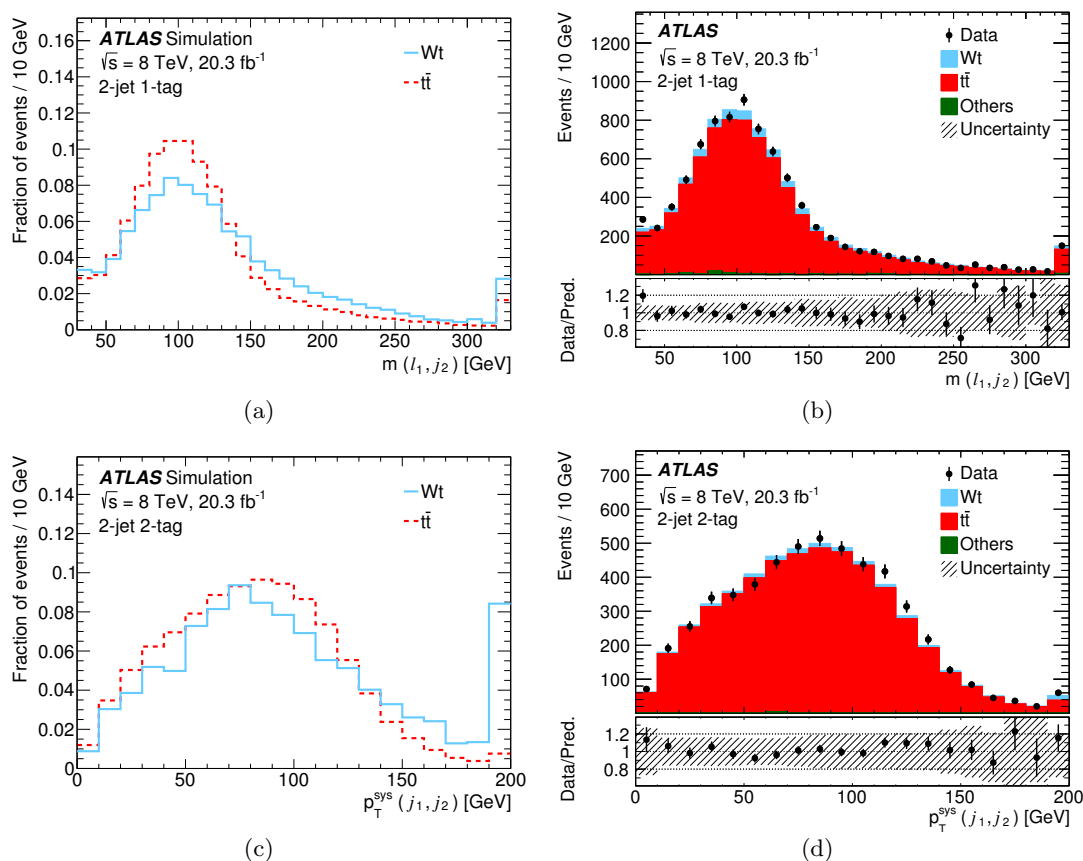
Figure 6. Distributions of the most important BDT input variables in the (a, b) 2-jet 1-tag and (c, d) 2-jet 2-tag regions. The distributions are shown for (a, b) the invariant mass of the system of the leading lepton and the second-leading jet and (c, d) the p_T of the system of the two jets. Each contribution is normalised to unit area in (a, c) and to its expectation in (b, d). The hatched area represents the sum in quadrature of the statistical and systematic uncertainties. The last bin includes the overflow.

to the modelling and the heavy-flavour correction, with an acceptance uncertainty for Wt and $t\bar{t}$ events of 1-2%. The shape uncertainty is taken into account for the JES component with the largest impact on the fit result (JES modelling component 1). The jet energy resolution uncertainty is evaluated by smearing the energy of each jet in the simulation and symmetrising the resulting change in acceptance and BDT response shape [79]. The resulting acceptance uncertainty for Wt and $t\bar{t}$ events is 1-3%, and the shape uncertainty is taken into account.

The uncertainties in the modelling of the jet reconstruction and the jet vertex fraction requirement are evaluated by randomly discarding jets according to the difference in jet reconstruction efficiency between the data and MC simulation and by varying the the jet vertex fraction requirement, respectively. These uncertainties have an impact on the acceptance for Wt and $t\bar{t}$ events of less than 1%. They do not change the shape of the BDT response.

Further uncertainties arise from the modelling of the trigger, reconstruction, and identification efficiencies for electrons [80] and muons [40], as well as from the modelling of
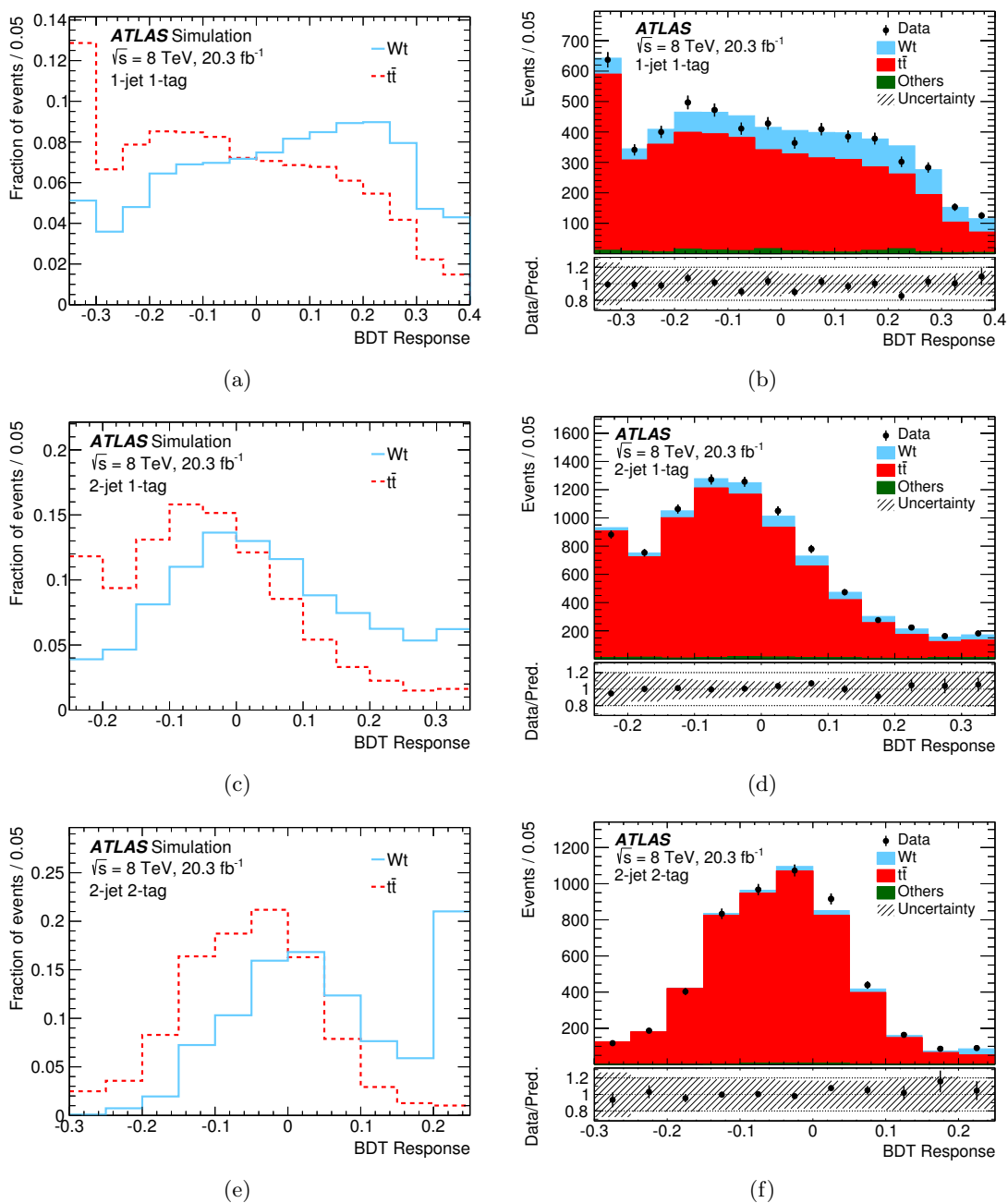
Figure 7. BDT response for (a, b) 1-jet 1-tag, (c, d) 2-jet 1-tag and (e, f) 2-jet 2-tag events. Each contribution is normalised to unit area in (a, c, e) and to its expectation in (b, d, f). The hatched area represents the sum in quadrature of the statistical and systematic uncertainties. The first bin includes the underflow and the last bin the overflow.

the electron and muon energy scale and resolution [40, 81]. These have an effect on the acceptance for Wt and $t\bar{t}$ events of less than 1%, except for the electron identification uncertainty, which has an acceptance uncertainty for Wt and $t\bar{t}$ of 2%. These uncertainties do not change the shape of the BDT response.

Uncertainties in the modelling of the b-tagging efficiency and mis-tag rates are estimated from data [47, 48]. These uncertainties depend on the jet flavour and p_T, and for mis-tag rates also on jet η. The uncertainty for b-jets is evaluated in six components, with the largest component having an acceptance uncertainty for Wt and $t\bar{t}$ events of 1–4%, depending on the analysis region [48]. The b-tag modelling uncertainties do not change the shape of the BDT response.

The variations in lepton and jet energies are propagated to the E_T^{miss} value. This uncertainty has additional contributions from the modelling of the energy deposits which are not associated with any reconstructed object [49]. Both an energy scale and an energy resolution component are considered. The corresponding acceptance uncertainty for Wt and $t\bar{t}$ events is less than 0.3%. The E_T^{miss} scale component also alters the shape of the BDT response.

Theoretical uncertainties are evaluated for the signal as well as the $t\bar{t}$ predictions. Figure 8 shows the relative shift of the BDT response associated with four of the theory modelling uncertainties. The uncertainty on the Wt signal and the $t\bar{t}$ background associated with initial- and final-state radiation (ISR/FSR) is evaluated using POWHEG-BOX interfaced to PYTHIA. The renormalisation scale associated with the strong coupling α_S is varied up and down by a factor of two in the matrix-element calculation and a PYTHIA Perugia 2012 tune is used to create samples with increased and decreased levels of radiation that are compatible with 7 TeV ATLAS data [82]. For $t\bar{t}$, the HDAMP parameter of POWHEG-BOX [51], which affects the amount of QCD radiation, is varied together with ISR/FSR. This uncertainty is treated as uncorrelated between Wt and $t\bar{t}$ events. Figure 8 shows that this uncertainty has a large effect on the acceptance and also alters the shape of the BDT response.

The uncertainty associated with the NLO matching method is evaluated by comparing POWHEG-BOX with MC@NLO, both interfaced to HERWIG. Figure 8 shows that this uncertainty has a dependence on the shape of the BDT response. For Wt production, the largest impact of this uncertainty is to shift events between the 1-jet 1-tag and 2-jet 2-tag regions. For $t\bar{t}$ events, the impact of this uncertainty is on the acceptance, where it is 11–12%. This uncertainty is treated as correlated between Wt and $t\bar{t}$ events.

The uncertainty associated with the modelling of the hadronisation and parton shower is evaluated by comparing samples where POWHEG-BOX is interfaced with PYTHIA to those where it is interfaced with HERWIG. This uncertainty alters the shape of the BDT response.

For the Wt signal, the uncertainty associated with the scheme used to remove overlap with $t\bar{t}$ is evaluated by comparing the two different schemes: the nominal sample, generated with the DR scheme, is compared to a sample generated with the DS scheme. The relative shift of the BDT response is shown in figure 8. The relative shift of this uncertainty is about 5% in the signal region for 1-jet 1-tag events, and grows to large values in the background-dominated region for 2-jet events, where its evaluation is limited by simulation statistics and the predicted event yield is very small. This uncertainty alters the shape of the BDT response.

The evaluation of the PDF uncertainty follows the PDF4LHC prescription [31] using three different PDF sets (CT10, MSTW2008NLO68CL [28] and NNPDF2.3 [32]). The
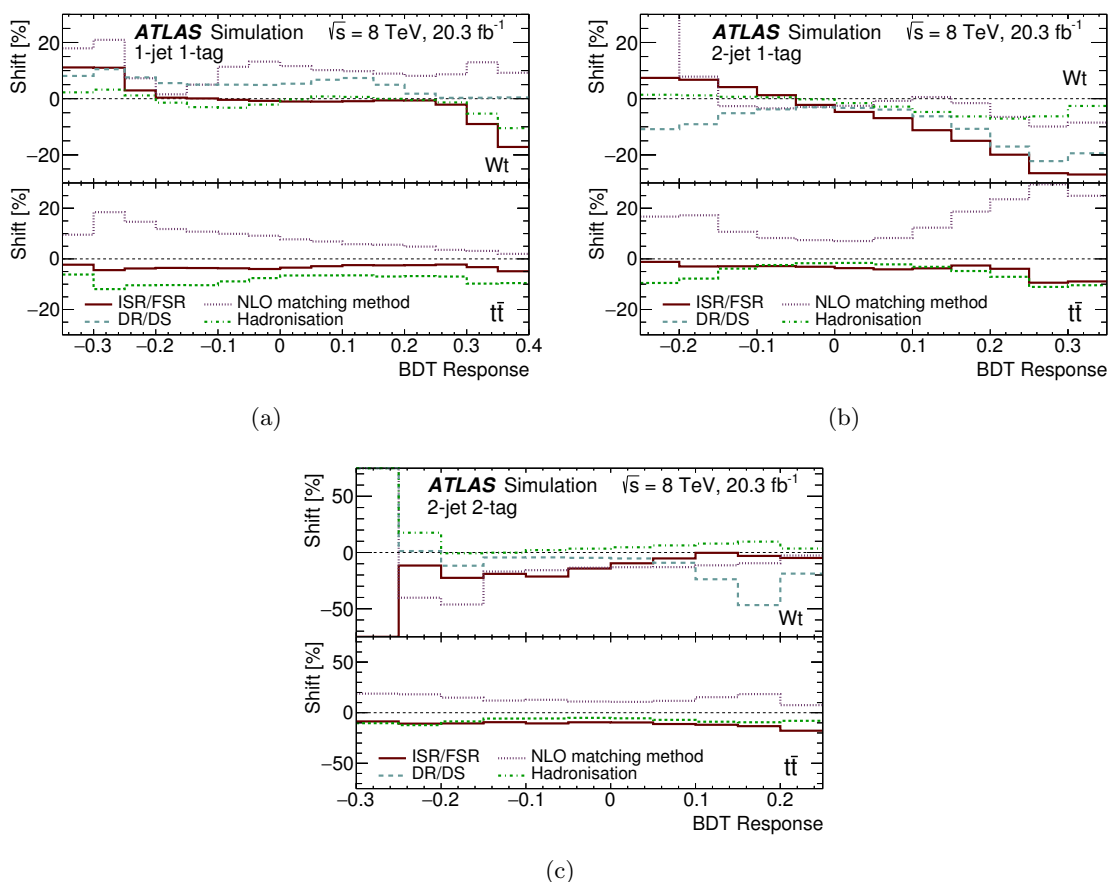
Figure 8. Relative shift of the BDT response associated with systematic variations of ISR/FSR, NLO matching method, DR/DS and hadronisation for (a) 1-jet 1-tag, (b) 2-jet 1-tag, and (c) 2-jet 2-tag events. DR refers to the diagram-removal scheme, DS to the diagram-subtraction scheme.

uncertainty on the acceptance for Wt and $t\bar{t}$ events is evaluated in each of the three analysis regions. The PDF uncertainty is considered correlated between Wt and $t\bar{t}$ events, except for $t\bar{t}$ 1-jet events, for which it is considered to be uncorrelated. The PDF uncertainty components that affect the $t\bar{t}$ acceptance in this region differ from the uncertainty components that affect the $t\bar{t}$ acceptance in the other regions [83].

The normalisation of the $t\bar{t}$ background has an uncertainty of 6% [65, 66]. The diboson background process has an uncertainty of 30% for 1-jet events and 40% for 2-jet events [84], which is treated as uncorrelated between different regions. The Z+jets and non-prompt or fake-lepton backgrounds have normalisation uncertainties of 60% to account for possible mismodelling of the jet multiplicity and the acceptance of these small backgrounds [85, 86]. The Z+jets and non-prompt or fake-lepton normalisation uncertainties are treated as uncorrelated between background sources and regions.

The uncertainty on the integrated luminosity is 2.8%. It is derived, following the same methodology as that detailed in ref. [87], from a preliminary calibration of the luminosity scale derived from beam-separation scans performed in November 2012. The luminosity uncertainty enters in the extraction of the cross-section as well as in the normalisation

of the background processes that are normalised to theory predictions. The statistical uncertainty due to the finite size of the simulation samples is also taken into account.

7 Results

7.1 Measurement of the inclusive cross-section

A profile likelihood fit to the BDT classifier distributions is performed, using the RooStats software [88, 89], in order to determine the inclusive Wt cross-section, utilising the 1-jet 1-tag, 2-jet 1-tag, and 2-jet 2-tag regions. The inclusion of the 2-jet regions provides additional signal sensitivity and also helps to constrain the $t\bar{t}$ background normalisation and systematic uncertainties.

The binned likelihood function is constructed as the product of Poisson probability terms over all bins considered in the analysis. This likelihood depends on the signal-strength parameter μ, which is a multiplicative factor on the unconstrained Wt yield prediction. Nuisance parameters (denoted θ) are used to encode the effects of the various sources of systematic uncertainty on the signal and background expectations. These nuisance parameters are implemented in the likelihood function with multiplicative Gaussian or log-normal constraints with mean θ_0 and standard deviation $\Delta\theta$. The likelihood is then maximised with respect to the full set of μ and θ parameters. The values of these parameters after maximisation are referred to as $\hat{\mu}$, $\hat{\theta}$, and $\Delta\hat{\theta}$.

The expected cross-section is obtained from a fit to the so-called Asimov dataset [90], with the signal and all backgrounds scaled to their predicted sizes [26]. The expected measurement is $\hat{\mu}_{\mathrm{exp}} = 1.00^{+0.17}_{-0.18}$. The observed result for the signal strength is $\hat{\mu}_{\mathrm{obs}} = 1.03^{+0.16}_{-0.17}$, which corresponds to a measured cross-section of $23.0 \pm 1.3\,(\mathrm{stat.})^{+3.2}_{-3.5}\,(\mathrm{syst.}) \pm 1.1\,(\mathrm{lumi.})\,\mathrm{pb}$. Including systematic uncertainties, the observed (expected) significance of the signal compared to the background-only hypothesis is 7.7 (6.9) standard deviations, obtained using an asymptotic approximation [90].

The post-fit (pre-fit) effect of each individual systematic uncertainty on $\hat{\mu}$ is calculated by fixing the corresponding nuisance parameter at $\hat{\theta} + \Delta\hat{\theta}$ ($\hat{\theta} + \Delta\theta$), and performing the fit again. The difference between the default and the modified $\hat{\mu}$, $\Delta\hat{\mu}$, represents the effect on $\hat{\mu}$ of this particular uncertainty. The pull $((\hat{\theta} - \theta_0)/\Delta\theta)$, and the pre-fit and post-fit impacts for the nuisance parameters with the largest impact on $\hat{\mu}$ are shown in figure 9. Since the total number of observed events in the 2-jet regions is about 14000, with a Wt signal fraction of about 6%, the nuisance parameters that have a $t\bar{t}$ acceptance uncertainty of more than about 2% can be constrained in the fit. This applies to the jet energy resolution and $t\bar{t}$ normalisation uncertainties, amongst others. The $E_{\mathrm{T}}^{\mathrm{miss}}$ scale uncertainty has a shape dependence in the 1-jet 1-tag region for Wt and $t\bar{t}$, which results in the corresponding nuisance parameter being shifted but not much constrained. The theory modelling uncertainties due to ISR/FSR, DR/DS, and NLO matching method have large pre-fit and post-fit impacts. The nuisance parameter for ISR/FSR Wt is shifted and constrained in the fit due to its BDT response shape dependence, shown in figure 8. This uncertainty has the largest impact on $\hat{\mu}$, both pre-fit and post-fit. The ISR/FSR $t\bar{t}$ uncertainty has a smaller post-fit impact on $\hat{\mu}$ and is constrained due its acceptance and
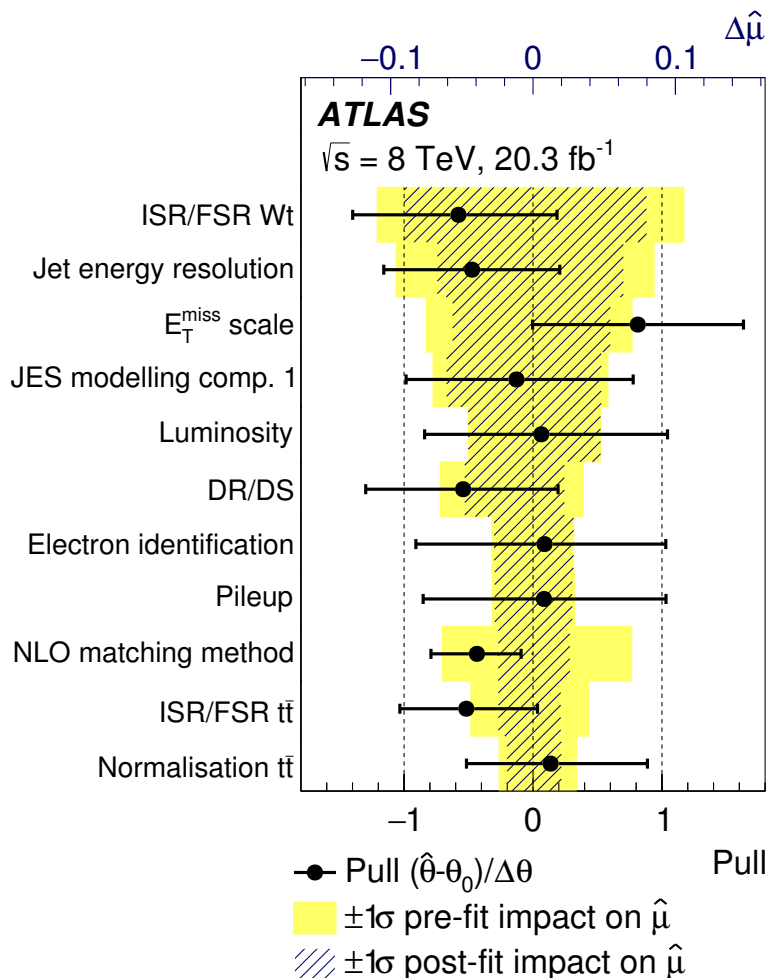
Figure 9. Effect on the uncertainty on the fitted value of the signal strength $\hat{\mu}$ ($\Delta\hat{\mu}$) and pull of the dominant nuisance parameters, ordered by their impact on $\hat{\mu}$. The shaded and hashed areas refer to the top axis: the shaded bands show the initial impact of that source of uncertainty on the precision of $\hat{\mu}$; the hatched areas show the impact on the measurement of that source of uncertainty, after the profile likelihood fit, at the $\pm 1\sigma$ level. The points and associated error bars show the pull of the nuisance parameters and their uncertainties and refer to the bottom axis. A mean of zero and a width of 1 would imply no constraint due to the profile likelihood fit. Only the 11 uncertainties with the largest impact on $\hat{\mu}$ are shown.

shape dependence. In a test where the ISR/FSR uncertainty is considered to be correlated between Wt and $t\bar{t}$ events, the expected uncertainty on $\hat{\mu}$ is reduced to ± 0.16. The nuisance parameter for the NLO matching method uncertainty is constrained by the $t\bar{t}$ background because of the large acceptance component and shape dependence of the NLO matching method uncertainty.

Table 4 summarises the contributions from the various sources of systematic uncertainty to the uncertainties on the observed fit result. The total uncertainty in the table is the uncertainty obtained from the full fit, and is therefore not identical to the sum in quadrature of the components, due to correlations that the fit induces between the uncer-

Uncertainty	Impact on $\hat{\mu}$ [%]
Statistical	± 5.8
Luminosity	± 4.7
Theory modelling	
ISR/FSR	$^{+8.2}_{-9.4}$
Hadronisation	± 1.7
NLO matching method	± 2.5
PDF	± 0.6
DR/DS	$^{+2.2}_{-4.8}$
Detector	
Jet	$^{+9.0}_{-9.9}$
Lepton	± 3.0
$E_{\mathrm{T}}^{\mathrm{miss}}$	± 5.5
b-tag	± 1.0
Background norm.	$^{+2.9}_{-2.6}$
Total	$^{+16}_{-17}$

Table 4. Summary of the relative uncertainties on the Wt cross-section measurement. Detector uncertainties are grouped into categories. All sources of uncertainty within a category are added in quadrature to obtain the category uncertainty.

tainties. The largest contributions to the cross-section uncertainty are from the modelling of ISR/FSR and from the jet energy resolution and scale.

The BDT response for each region is shown normalised to the fit result in figure 10. The dependence of the cross-section on the top-quark mass is evaluated using Wt and $t\bar{t}$ simulation samples with various top-quark masses. The cross-section depends linearly on the top-quark mass due to changes in acceptance, with a slope of 1.11 pb/GeV.

7.2 Constraints on $|f_{\mathrm{LV}}V_{tb}|$ and $|V_{tb}|$

The inclusive cross-section measurement provides a direct determination of the magnitude of the CKM matrix element V_{tb}. The ratio of the measured cross-section to the theoretical prediction is equal to $|f_{\mathrm{LV}}V_{tb}|^2$, where the form factor f_{LV} could be modified by new physics or radiative corrections through anomalous coupling contributions, for example those in refs. [3, 91, 92]. The Wt production and top-quark decays through $|V_{ts}|$ and $|V_{td}|$ are assumed to be small. A lower limit on $|V_{tb}|$ is obtained for $f_{\mathrm{LV}} = 1$ as in the SM, without assuming CKM unitarity [5, 93]. An additional systematic uncertainty due to a variation of the top-quark mass by 1 GeV is included in the V_{tb} extraction. The uncertainties on the theoretical cross-section due to the variation of the renormalisation and factorisation scale (0.6 pb), the PDF uncertainty (1.4 pb), and the beam-energy uncertainty [94] (0.38 pb) are also accounted for.

The value for $|f_{\mathrm{LV}}V_{tb}|$ is extracted from the $|f_{\mathrm{LV}}V_{tb}|^2$ likelihood, which is assumed to be Gaussian. The lower limit on $|V_{tb}|^2$ corresponds to 95% of the integral of this likelihood,
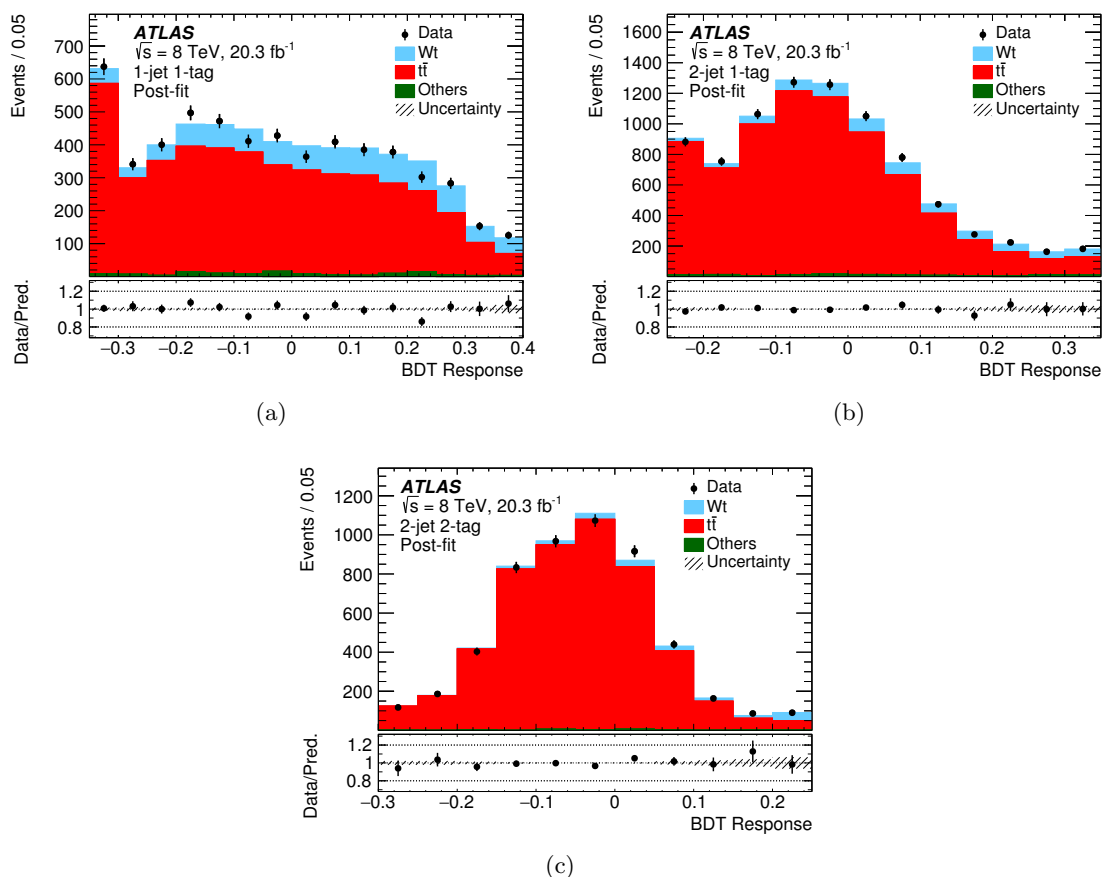
Figure 10. Distribution of the post-fit BDT response for (a) 1-jet 1-tag, (b) 2-jet 1-tag, and (c) 2-jet 2-tag events. The signal, backgrounds and uncertainties are scaled to the fit result. The first bin includes the underflow and the last bin the overflow.

setting $f_{LV} = 1$ and starting at 1. The measured value of $|f_{LV}V_{tb}|$ is 1.01 ± 0.10, and the corresponding lower limit on $|V_{tb}|$ at the 95% confidence level is 0.80.

8 Cross-section measurement inside a fiducial acceptance

The cross-section for the production of events containing a top quark and a W boson is measured in a fiducial region to allow a more robust comparison to the theoretical prediction without extrapolating to regions outside of the detector acceptance. The fiducial measurement reduces the sensitivity of the cross-section to theory modelling uncertainties. The measurement can also be compared to particle-level predictions for the inclusive WWb and $WWbb$ processes at NLO, once those calculations become available [36, 95]. The fiducial acceptance requires two leptons and exactly one b-jet at the particle level. This encompasses not only Wt production but also $t\bar{t}$ production where one of the b-quarks from the top-quark decays is not in the particle-level acceptance. The fiducial cross-section is measured by fitting the sum of the Wt and $t\bar{t}$ contributions to data in the 1-jet 1-tag region. Control regions are not used in the fit.

Process	Particle-level selection	Detector-level selection	
		in-fiducial	out-of-fiducial
Wt	4200(100)	810(160)	230(40)
$t\bar{t}$	12 000(2000)	2400(500)	2100(400)

Table 5. Number of expected events at the particle-level and for the detector-level selection for Wt and $t\bar{t}$. The uncertainty for the particle-level includes ISR/FSR, NLO matching method, and for Wt also hadronisation, all added in quadrature. The uncertainty for the detector-level selection includes all sources of uncertainty, added in quadrature.

8.1 Fiducial selection

The definition of the fiducial acceptance is based on MC simulation and uses particle-level physics objects constructed of stable particles with a mean lifetime $\tau > 0.3 \times 10^{-10}$ s. Electrons and muons are required to originate from W-boson decays, either directly or via leptonically decaying τ leptons. The p_{T} of each of the leptons is corrected by adding the energy and momentum of photons inside a cone of size $\Delta R = 0.1$ around the lepton direction. Electrons and muons are required to have $p_{\mathrm{T}} > 25$ GeV and $|\eta| < 2.5$. Jets are clustered from particles using the anti-k_t algorithm with radius parameter $R = 0.4$. Neutrinos, electrons and muons from W-boson decays as well as particles resulting from pileup are excluded from jet clustering. Particles from the underlying event are included. The particle-level jets are required to have $p_{\mathrm{T}} > 20$ GeV and $|\eta| < 2.5$ and are matched with nearby b-hadrons with a p_{T} of at least 5 GeV using the ghost tagging method [96]. Jets within $\Delta R = 0.2$ of the nearest electron are removed from the list. Following that, electrons and muons within $\Delta R = 0.4$ of the nearest jet are removed. Missing transverse momentum is calculated using neutrinos from W-boson decays. The Wt and $t\bar{t}$ events pass the fiducial selection if they have exactly two leptons, exactly one b-jet and $E_{\mathrm{T}}^{\mathrm{miss}} > 20$ GeV. The numbers of simulated Wt and $t\bar{t}$ events passing this fiducial selection are shown in table 5, and Wt production contributes 26% of these particle-level events.

Simulated Wt and $t\bar{t}$ events that satisfy the detector-level selection criteria are separated into two categories: in-fiducial (satisfying the fiducial selection criteria) and out-of-fiducial (the rest). Table 5 shows the number of events for Wt and $t\bar{t}$ in each category. The Wt contribution is 25% of the in-fiducial events, but only 10% of the out-of-fiducial events. The out-of-fiducial events that pass the detector-level selection typically have two or more particle-level jets, only one of which is also reconstructed at the detector level. Thus the $t\bar{t}$ contribution to the out-of-fiducial events is larger.

8.2 Systematic uncertainties

The sources of systematic uncertainty in the inclusive cross-section measurement are also considered for the fiducial measurement. The object reconstruction and background-normalisation uncertainties also apply in this measurement (except the $t\bar{t}$ normalisation uncertainty, as discussed below). For in-fiducial events, a variation in the theory modelling uncertainties (DR/DS, ISR/FSR, hadronisation, NLO matching method, and PDF) changes the detector-level and fiducial acceptances in the same direction, which reduces the

Uncertainty	Impact on $\hat{\mu}_{\text{fid}}$ [%]
Statistical	1.0
Luminosity	3.1
Theory modelling	
ISR/FSR	4.2
Hadronisation	0.8
NLO matching method	0.7
PDF	¡0.1
Ratio $Wt/t\bar{t}$	2.2
DR/DS	0.1
Detector	
Jet	5.2
Lepton	2.3
$E_{\text{T}}^{\text{miss}}$	0.2
b-tag	2.3
Background norm.	< 0.1
Total	8.2

Table 6. Summary of the uncertainties on the observed fit result for the fiducial cross-section. Detector uncertainties are grouped into categories. All sources of uncertainty within a category are added in quadrature to obtain the category uncertainty.

impact of these uncertainties. Since this does not affect out-of-fiducial events, these theory modelling uncertainties are treated as uncorrelated between in- and out-of-fiducial events.

An additional uncertainty accounts for the relative fractions of Wt and $t\bar{t}$ due to the uncertainty on the theoretical predictions. The fraction of each type of signal is allowed to vary within their theoretical predictions, keeping the sum constant.

8.3 Results

The fiducial cross-section is measured in a profile likelihood fit to data in the 1-jet 1-tag region. In-fiducial and out-of-fiducial Wt and $t\bar{t}$ events are scaled by the same cross-section scale factor μ_{fid} in the fit. The measured fiducial cross-section for Wt and $t\bar{t}$ production is $0.85 \pm 0.01\,(\text{stat.})^{+0.06}_{-0.07}\,(\text{syst.}) \pm 0.03\,(\text{lumi.})$ pb, which corresponds to a total uncertainty of 8%. The expected uncertainty is also 8%. The impact of the systematic uncertainties on this measurement is summarised in table 6. The relative uncertainties are smaller in the fiducial measurement than in the inclusive measurement (cf. table 4) because both Wt and $t\bar{t}$ events are considered signal and because of the definition of the fiducial acceptance. The only exception is the b-tag uncertainty, which is larger in the fiducial measurement because only 1-jet 1-tag events are used in the fit.

The measured fiducial cross-section is compared to theoretical predictions for the sum of the fiducial Wt and $t\bar{t}$ cross-sections in figure 11. The uncertainty on the theory predictions accounts for scale and PDF contributions. The MSTW2008 and NNPDF2.3 predictions are obtained by re-weighting the simulated Mc@nlo sample. The uppermost result
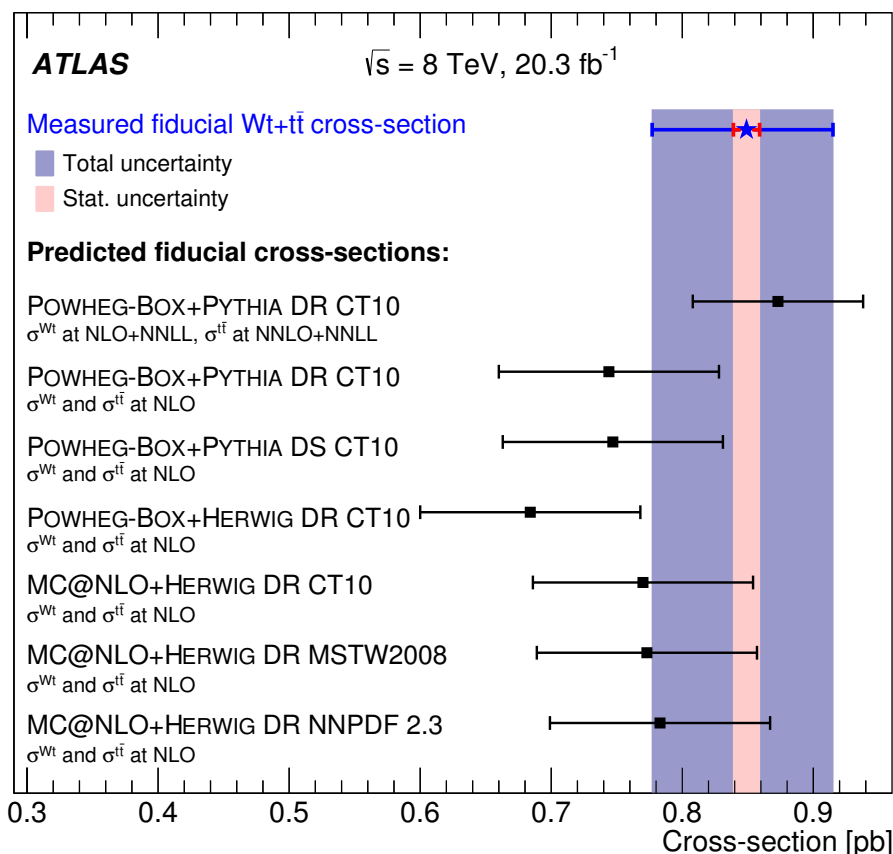
Figure 11. Comparison of the measured fiducial cross-section to theoretical predictions in a fiducial acceptance requiring two leptons with $p_{\mathrm{T}} > 25$ GeV and $|\eta| < 2.5$, one jet with $p_{\mathrm{T}} > 20$ GeV and $|\eta| < 2.5$, and $E_{\mathrm{T}}^{\mathrm{miss}} > 20$ GeV. The predictions are computed at NLO accuracy for the fiducial acceptance and the inclusive cross-section, except for the top line, for which the inclusive cross-sections for Wt and $t\bar{t}$ are computed at NLO+NNLL and NNLO+NNLL accuracy, respectively.

for the predicted fiducial cross-section is based on the fiducial acceptances and the sample normalisation utilised in this analysis. The fiducial acceptances are computed from the nominal POWHEG-BOX+PYTHIA samples. The Wt and $t\bar{t}$ cross-sections are normalised to their NLO+NNLL and NNLO+NNLL predictions, respectively. The other results utilise the theoretical cross-sections as computed by the respective generator.

9 Conclusion

The inclusive cross-section for the production of a single top quark in association with a W boson has been measured in proton-proton collisions at a centre-of-mass energy of 8 TeV, using dilepton events from $20.3\,\mathrm{fb}^{-1}$ of data recorded by the ATLAS detector at the LHC. Wt production is observed with a significance of 7.7 σ. The measured cross-section is

$$23.0 \pm 1.3\,(\mathrm{stat.})^{+3.2}_{-3.5}\,(\mathrm{syst.}) \pm 1.1\,(\mathrm{lumi.})\ \mathrm{pb}\,,$$

in agreement with the NLO+NNLL expectation. The measured cross-section is used to extract a direct measurement of the left-handed form factor times the CKM matrix element $|f_{\rm LV}V_{tb}|$ of 1.01 ± 0.10. The lower limit on $|V_{tb}|$ is 0.80 at the 95% CL, without assuming unitarity of the CKM matrix. The cross-section for the production of a W boson and a top quark (including Wt and $t\bar{t}$) has also been measured in a fiducial acceptance requiring two leptons with $p_{\rm T} > 25$ GeV and $|\eta| < 2.5$, one jet with $p_{\rm T} > 20$ GeV and $|\eta| < 2.5$, and $E_{\rm T}^{\rm miss} > 20$ GeV. The fiducial cross-section is

$$0.85 \pm 0.01\,({\rm stat.})^{+0.06}_{-0.07}\,({\rm syst.}) \pm 0.03\,({\rm lumi.})\,{\rm pb}\,.$$

References

[1] N. Cabibbo, *Unitary symmetry and leptonic decays*, *Phys. Rev. Lett.* **10** (1963) 531.

[2] M. Kobayashi and T. Maskawa, *CP-violation in the renormalizable theory of weak interaction*, *Prog. Theor. Phys.* **49** (1973) 652.

[3] G.L. Kane et al., *Using the top quark for testing standard model polarization and CP predictions*, *Phys. Rev.* **D 45** (1992) 124.

[4] D0 collaboration, V.M. Abazov et al., *Combination of searches for anomalous top quark couplings with $5.4\,fb^{-1}$ of $p\bar{p}$ collisions*, *Phys. Lett.* **B 713** (2012) 165 [arXiv:1204.2332] [ɪɴSPIRE].

[5] J. Alwall et al., *Is $V_{tb} \simeq 1$?*, *Eur. Phys. J.* **C 49** (2007) 791 [hep-ph/0607115] [ɪɴSPIRE].

[6] T.M.P. Tait and C.P. Yuan, *Single top quark production as a window to physics beyond the standard model*, *Phys. Rev.* **D 63** (2000) 014018 [hep-ph/0007298] [ɪɴSPIRE].

[7] Q.-H. Cao, J. Wudka and C.P. Yuan, *Search for new physics via single top production at the LHC*, *Phys. Lett.* **B 658** (2007) 50 [arXiv:0704.2809] [ɪɴSPIRE].

[8] J. Nutter, R. Schwienhorst, D.G.E. Walker and J.-H. Yu, *Single top production as a probe of B-prime quarks*, *Phys. Rev.* **D 86** (2012) 094006 [arXiv:1207.5179] [ɪɴSPIRE].

[9] ATLAS collaboration, *Search for single b^*-quark production with the ATLAS detector at $\sqrt{s} = 7$ TeV*, *Phys. Lett.* **B 721** (2013) 171 [arXiv:1301.1583] [ɪɴSPIRE].

[10] D0 collaboration, V.M. Abazov et al., *Model-independent measurement of t-channel single top quark production in $p\bar{p}$ collisions at $\sqrt{s} = 1.96$ TeV*, *Phys. Lett.* **B 705** (2011) 313 [arXiv:1105.2788] [ɪɴSPIRE].

[11] CDF, D0 collaboration, T.A. Aaltonen et al., *Tevatron combination of single-top-quark cross sections and determination of the magnitude of the Cabibbo-Kobayashi-Maskawa matrix element V_{tb}*, *Phys. Rev. Lett.* **115** (2015) 152003 [arXiv:1503.05027] [ɪɴSPIRE].

[12] D0 collaboration, V.M. Abazov et al., *Evidence for s-channel single top quark production in $p\bar{p}$ collisions at $\sqrt{s} = 1.96$ TeV*, *Phys. Lett.* **B 726** (2013) 656 [arXiv:1307.0731] [ɪɴSPIRE].

[13] CDF collaboration, T.A. Aaltonen et al., *Evidence for s-channel single-top-quark production in events with one charged lepton and two jets at CDF*, *Phys. Rev. Lett.* **112** (2014) 231804 [arXiv:1402.0484] [ɪɴSPIRE].

[14] CDF, D0 collaboration, T.A. Aaltonen et al., *Observation of s-channel production of single top quarks at the Tevatron*, *Phys. Rev. Lett.* **112** (2014) 231803 [arXiv:1402.5126] [ɪɴSPIRE].

[15] CDF collaboration, T. Aaltonen et al., *First observation of electroweak single top quark production*, *Phys. Rev. Lett.* **103** (2009) 092002 [arXiv:0903.0885] [ɪɴSPIRE].

[16] D0 collaboration, V.M. Abazov et al., *Observation of single top quark production*, *Phys. Rev. Lett.* **103** (2009) 092001 [arXiv:0903.0850] [ɪɴSPIRE].

[17] CDF, D0 collaboration, T.E.W. Group, *Combination of CDF and D0 measurements of the single top production cross section*, arXiv:0908.2171 [ɪɴSPIRE].

[18] ATLAS collaboration, *Measurement of the t-channel single top-quark production cross section in pp collisions at $\sqrt{s} = 7$ TeV with the ATLAS detector*, *Phys. Lett.* **B 717** (2012) 330 [arXiv:1205.3130] [ɪɴSPIRE].

[19] ATLAS collaboration, *Comprehensive measurements of t-channel single top-quark production cross sections at $\sqrt{s} = 7$ TeV with the ATLAS detector*, *Phys. Rev.* **D 90** (2014) 112006 [arXiv:1406.7844] [INSPIRE].

[20] CMS collaboration, *Measurement of the single-top-quark t-channel cross section in pp collisions at $\sqrt{s} = 7$ TeV*, *JHEP* **12** (2012) 035 [arXiv:1209.4533] [INSPIRE].

[21] CMS collaboration, *Measurement of the t-channel single-top-quark production cross section and of the $|V_{tb}|$ CKM matrix element in pp collisions at $\sqrt{s} = 8$ TeV*, *JHEP* **06** (2014) 090 [arXiv:1403.7366] [INSPIRE].

[22] ATLAS collaboration, *Search for s-channel single top-quark production in proton-proton collisions at $\sqrt{s} = 8$ TeV with the ATLAS detector*, *Phys. Lett.* **B 740** (2015) 118 [arXiv:1410.0647] [INSPIRE].

[23] ATLAS collaboration, *Evidence for the associated production of a W boson and a top quark in ATLAS at $\sqrt{s} = 7$ TeV*, *Phys. Lett.* **B 716** (2012) 142 [arXiv:1205.5764] [INSPIRE].

[24] CMS collaboration, *Evidence for associated production of a single top quark and W boson in pp collisions at $\sqrt{s} = 7$ TeV*, *Phys. Rev. Lett.* **110** (2013) 022003 [arXiv:1209.3489] [INSPIRE].

[25] CMS collaboration, *Observation of the associated production of a single top quark and a W boson in pp collisions at $\sqrt{s} = 8$ TeV*, *Phys. Rev. Lett.* **112** (2014) 231802 [arXiv:1401.2942] [INSPIRE].

[26] N. Kidonakis, *Two-loop soft anomalous dimensions for single top quark associated production with a W^- or H^-*, *Phys. Rev.* **D 82** (2010) 054018 [arXiv:1005.4451] [INSPIRE].

[27] ATLAS, CDF, CMS, D0 collaboration, *First combination of Tevatron and LHC measurements of the top-quark mass*, arXiv:1403.4427 [INSPIRE].

[28] A.D. Martin, W.J. Stirling, R.S. Thorne and G. Watt, *Parton distributions for the LHC*, *Eur. Phys. J.* **C 63** (2009) 189 [arXiv:0901.0002] [INSPIRE].

[29] M. Aliev, H. Lacker, U. Langenfeld, S. Moch, P. Uwer and M. Wiedermann, *HATHOR: HAdronic Top and Heavy quarks crOss section calculatoR*, *Comput. Phys. Commun.* **182** (2011) 1034 [arXiv:1007.1327] [INSPIRE].

[30] P. Kant et al., *HatHor for single top-quark production: Updated predictions and uncertainty estimates for single top-quark production in hadronic collisions*, *Comput. Phys. Commun.* **191** (2015) 74 [arXiv:1406.4403] [INSPIRE].

[31] M. Botje et al., *The PDF4LHC working group interim recommendations*, arXiv:1101.0538 [INSPIRE].

[32] NNPDF collaboration, R.D. Ball et al., *Parton distributions with QED corrections*, *Nucl. Phys.* **B 877** (2013) 290 [arXiv:1308.0598] [INSPIRE].

[33] J.H. Friedman, *Stochastic gradient boosting*, *Comput. Stat. Data Anal.* **38** (2002) 367.

[34] J.M. Campbell and F. Tramontano, *Next-to-leading order corrections to Wt production and decay*, *Nucl. Phys.* **B 726** (2005) 109 [hep-ph/0506289] [INSPIRE].

[35] S. Frixione, E. Laenen, P. Motylinski and B.R. Webber, *Single-top production in MC@NLO*, *JHEP* **03** (2006) 092 [hep-ph/0512250] [INSPIRE].

[36] F. Cascioli, S. Kallweit, P. Maierhöfer and S. Pozzorini, *A unified NLO description of top-pair and associated Wt production*, *Eur. Phys. J.* **C 74** (2014) 2783 [arXiv:1312.0546] [INSPIRE].

[37] ATLAS collaboration, *The ATLAS experiment at the CERN Large Hadron Collider*, 2008 *JINST* **3** S08003.

[38] ATLAS collaboration, *Performance of the ATLAS Trigger System in 2010*, *Eur. Phys. J.* **C 72** (2012) 1849 [arXiv:1110.1530] [InSPIRE].

[39] ATLAS collaboration, *Electron reconstruction and identification efficiency measurements with the ATLAS detector using the 2011 LHC proton-proton collision data*, *Eur. Phys. J.* **C 74** (2014) 2941 [arXiv:1404.2240] [InSPIRE].

[40] ATLAS collaboration, *Measurement of the muon reconstruction performance of the ATLAS detector using 2011 and 2012 LHC proton-proton collision data*, *Eur. Phys. J.* **C 74** (2014) 3130 [arXiv:1407.3935] [InSPIRE].

[41] K. Rehermann and B. Tweedie, *Efficient identification of boosted semileptonic top quarks at the LHC*, *JHEP* **03** (2011) 059 [arXiv:1007.2221] [InSPIRE].

[42] G.P. Salam and G. Soyez, *A practical seedless infrared-safe cone jet algorithm*, *JHEP* **05** (2007) 086 [arXiv:0704.0292] [InSPIRE].

[43] W. Lampl, *Calorimeter clustering algorithms: description and performance*, ATL-LARG-PUB-2008-002 (2008).

[44] ATLAS collaboration, *Jet energy measurement with the ATLAS detector in proton-proton collisions at $\sqrt{s} = 7$ TeV*, *Eur. Phys. J.* **C 73** (2013) 2304 [arXiv:1112.6426] [InSPIRE].

[45] ATLAS collaboration, *Tagging and suppression of pileup jets with the ATLAS detector*, ATLAS-CONF-2014-018 (2014).

[46] ATLAS collaboration, *Commissioning of the ATLAS high-performance b-tagging algorithms in the 7 TeV collision data*, ATLAS-CONF-2011-102 (2011).

[47] ATLAS collaboration, *Calibration of the performance of b-tagging for c and light-flavour jets in the 2012 ATLAS data*, ATLAS-CONF-2014-046 (2014).

[48] ATLAS collaboration, *Calibration of b-tagging using dileptonic top pair events in a combinatorial likelihood approach with the ATLAS experiment*, ATLAS-CONF-2014-004 (2014).

[49] ATLAS collaboration, *Performance of missing transverse momentum reconstruction in proton-proton collisions at 7 TeV with ATLAS*, *Eur. Phys. J.* **C 72** (2012) 1844 [arXiv:1108.5602] [InSPIRE].

[50] S. Alioli, S.-O. Moch and P. Uwer, *Hadronic top-quark pair-production with one jet and parton showering*, *JHEP* **01** (2012) 137 [arXiv:1110.5251] [InSPIRE].

[51] S. Alioli, P. Nason, C. Oleari and E. Re, *A general framework for implementing NLO calculations in shower Monte Carlo programs: the POWHEG BOX*, *JHEP* **06** (2010) 043 [arXiv:1002.2581] [InSPIRE].

[52] T. Sjöstrand, S. Mrenna and P.Z. Skands, *PYTHIA 6.4 physics and manual*, *JHEP* **05** (2006) 026 [hep-ph/0603175] [InSPIRE].

[53] P.Z. Skands, *Tuning Monte Carlo generators: the Perugia tunes*, *Phys. Rev.* **D 82** (2010) 074018 [arXiv:1005.3457] [InSPIRE].

[54] H.-L. Lai et al., *New parton distributions for collider physics*, *Phys. Rev.* **D 82** (2010) 074024 [arXiv:1007.2241] [InSPIRE].

[55] P.M. Nadolsky et al., *Implications of CTEQ global analysis for collider observables*, *Phys. Rev.* **D 78** (2008) 013004 [arXiv:0802.0007] [INSPIRE].

[56] S. Frixione, E. Laenen, P. Motylinski, B.R. Webber and C.D. White, *Single-top hadroproduction in association with a W boson*, *JHEP* **07** (2008) 029 [arXiv:0805.3067] [INSPIRE].

[57] S. Frixione and B.R. Webber, *Matching NLO QCD computations and parton shower simulations*, *JHEP* **06** (2002) 029 [hep-ph/0204244] [INSPIRE].

[58] G. Corcella et al., *HERWIG 6: an event generator for hadron emission reactions with interfering gluons (including supersymmetric processes)*, *JHEP* **01** (2001) 010 [hep-ph/0011363] [INSPIRE].

[59] J.M. Butterworth, J.R. Forshaw and M.H. Seymour, *Multiparton interactions in photoproduction at HERA*, *Z. Phys.* **C 72** (1996) 637 [hep-ph/9601371] [INSPIRE].

[60] M. Cacciari, M. Czakon, M. Mangano, A. Mitov and P. Nason, *Top-pair production at hadron colliders with next-to-next-to-leading logarithmic soft-gluon resummation*, *Phys. Lett.* **B 710** (2012) 612 [arXiv:1111.5869] [INSPIRE].

[61] M. Beneke, P. Falgari, S. Klein and C. Schwinn, *Hadronic top-quark pair production with NNLL threshold resummation*, *Nucl. Phys.* **B 855** (2012) 695 [arXiv:1109.1536] [INSPIRE].

[62] P. Bärnreuther, M. Czakon and A. Mitov, *Percent level precision physics at the Tevatron: first genuine NNLO QCD corrections to $q\bar{q} \to t\bar{t} + X$*, *Phys. Rev. Lett.* **109** (2012) 132001 [arXiv:1204.5201] [INSPIRE].

[63] M. Czakon and A. Mitov, *NNLO corrections to top-pair production at hadron colliders: the all-fermionic scattering channels*, *JHEP* **12** (2012) 054 [arXiv:1207.0236] [INSPIRE].

[64] M. Czakon and A. Mitov, *NNLO corrections to top pair production at hadron colliders: the quark-gluon reaction*, *JHEP* **01** (2013) 080 [arXiv:1210.6832] [INSPIRE].

[65] M. Czakon, P. Fiedler and A. Mitov, *Total top-quark pair-production cross section at hadron colliders through $O(\alpha_S^4)$*, *Phys. Rev. Lett.* **110** (2013) 252004 [arXiv:1303.6254] [INSPIRE].

[66] M. Czakon and A. Mitov, *Top++: a program for the calculation of the top-pair cross-section at hadron colliders*, *Comput. Phys. Commun.* **185** (2014) 2930 [arXiv:1112.5675] [INSPIRE].

[67] M.L. Mangano, M. Moretti, F. Piccinini, R. Pittau and A.D. Polosa, *ALPGEN, a generator for hard multiparton processes in hadronic collisions*, *JHEP* **07** (2003) 001 [hep-ph/0206293] [INSPIRE].

[68] J.M. Campbell and R.K. Ellis, *An update on vector boson pair production at hadron colliders*, *Phys. Rev.* **D 60** (1999) 113006 [hep-ph/9905386] [INSPIRE].

[69] K. Melnikov and F. Petriello, *Electroweak gauge boson production at hadron colliders through $O(\alpha_s^2)$*, *Phys. Rev.* **D 74** (2006) 114017 [hep-ph/0609070] [INSPIRE].

[70] ATLAS collaboration, *Estimation of non-prompt and fake lepton backgrounds in final states with top quarks produced in proton-proton collisions at $\sqrt{s} = 8$ TeV with the ATLAS detector*, ATLAS-CONF-2014-058 (2014).

[71] ATLAS collaboration, *The ATLAS simulation infrastructure*, *Eur. Phys. J.* **C 70** (2010) 823 [arXiv:1005.4568] [INSPIRE].

[72] GEANT4 collaboration, S. Agostinelli, *GEANT4: a simulation toolkit*, *Nucl. Instrum. Meth.* **A 506** (2003) 250.

[73] A. Hocker et al., *TMVA — Toolkit for Multivariate Data Analysis*, PoS(ACAT)040 [physics/0703039] [INSPIRE].

[74] Y. Freund and R.E. Schapire, *A decision-theoretic generalization of on-line learning and an application to boosting*, *J. Comput. Syst. Sci.* **55** (1997) 119.

[75] C.G. Lester and D.J. Summers, *Measuring masses of semiinvisibly decaying particles pair produced at hadron colliders*, *Phys. Lett.* **B 463** (1999) 99 [hep-ph/9906349] [INSPIRE].

[76] A. Barr, C. Lester and P. Stephens, *m(T2): the truth behind the glamour*, *J. Phys.* **G 29** (2003) 2343 [hep-ph/0304226] [INSPIRE].

[77] H.-C. Cheng and Z. Han, *Minimal kinematic constraints and m(T2)*, *JHEP* **12** (2008) 063 [arXiv:0810.5178] [INSPIRE].

[78] ATLAS collaboration, *Jet energy measurement and its systematic uncertainty in proton-proton collisions at $\sqrt{s} = 7$ TeV with the ATLAS detector*, *Eur. Phys. J.* **C 75** (2015) 17 [arXiv:1406.0076] [INSPIRE].

[79] ATLAS collaboration, *Jet energy resolution in proton-proton collisions at $\sqrt{s} = 7$ TeV recorded in 2010 with the ATLAS detector*, *Eur. Phys. J.* **C 73** (2013) 2306 [arXiv:1210.6210] [INSPIRE].

[80] ATLAS collaboration, *Electron efficiency measurements with the ATLAS detector using the 2012 LHC proton-proton collision data*, ATLAS-CONF-2014-032 (2014).

[81] ATLAS collaboration, *Electron and photon energy calibration with the ATLAS detector using LHC Run 1 data*, *Eur. Phys. J.* **C 74** (2014) 3071 [arXiv:1407.5063] [INSPIRE].

[82] ATLAS collaboration, *Measurement of $t\bar{t}$ production with a veto on additional central jet activity in pp collisions at $\sqrt{s} = 7$ TeV using the ATLAS detector*, *Eur. Phys. J.* **C 72** (2012) 2043 [arXiv:1203.5015] [INSPIRE].

[83] ATLAS collaboration, *Study of correlation of PDF uncertainty in single top and top pair production at the LHC*, ATL-PHYS-PUB-2015-010 (2015).

[84] C. Anastasiou, L.J. Dixon, K. Melnikov and F. Petriello, *High precision QCD at hadron colliders: electroweak gauge boson rapidity distributions at NNLO*, *Phys. Rev.* **D 69** (2004) 094008 [hep-ph/0312266] [INSPIRE].

[85] C.F. Berger et al., *Precise predictions for W + 4 jet production at the Large Hadron Collider*, *Phys. Rev. Lett.* **106** (2011) 092001 [arXiv:1009.2338] [INSPIRE].

[86] F.A. Berends, H. Kuijf, B. Tausk and W.T. Giele, *On the production of a W and jets at hadron colliders*, *Nucl. Phys.* **B 357** (1991) 357.

[87] ATLAS collaboration, *Improved luminosity determination in pp collisions at $\sqrt{s} = 7$ TeV using the ATLAS detector at the LHC*, *Eur. Phys. J.* **C 73** (2013) 2518 [arXiv:1302.4393] [INSPIRE].

[88] (NIKHEF, Amsterdam), *HistFactory: a tool for creating statistical models for use with RooFit and RooStats*, CERN-OPEN-2012-016 (2012).

[89] L. Moneta et al., *The RooStats Project*, PoS(ACAT2010)057 [arXiv:1009.1003] [INSPIRE].

[90] G. Cowan, K. Cranmer, E. Gross and O. Vitells, *Asymptotic formulae for likelihood-based tests of new physics*, *Eur. Phys. J.* **C 71** (2011) 1554 [*Erratum ibid.* **C 73** (2013) 2501] [arXiv:1007.1727] [INSPIRE].

[91] J.A. Aguilar-Saavedra, *A minimal set of top anomalous couplings*, [*Nucl. Phys.* **B 812** (2009)](https://doi.org/) 181 [[arXiv:0811.3842](https://arxiv.org/abs/0811.3842)] [INSPIRE].

[92] T.G. Rizzo, *Single top quark production as a probe for anomalous moments at hadron colliders*, [*Phys. Rev.* **D 53** (1996) 6218](https://doi.org/) [[hep-ph/9506351](https://arxiv.org/abs/hep-ph/9506351)] [INSPIRE].

[93] Q.-H. Cao and B. Yan, *Determining V_{tb} at electron-positron colliders*, [*Phys. Rev.* **D 92** (2015) 094018](https://doi.org/) [[arXiv:1507.06204](https://arxiv.org/abs/1507.06204)] [INSPIRE].

[94] J. Wenninger, *Energy calibration of the LHC beams at 4 TeV*, [CERN-ATS-2013-040](https://doi.org/) (2013).

[95] G. Heinrich, A. Maier, R. Nisius, J. Schlenk and J. Winter, *NLO QCD corrections to $W^+W^-b\bar{b}$ production with leptonic decays in the light of top quark mass and asymmetry measurements*, [*JHEP* **06** (2014) 158](https://doi.org/) [[arXiv:1312.6659](https://arxiv.org/abs/1312.6659)] [INSPIRE].

[96] S. Schaetzel and M. Spannowsky, *Tagging highly boosted top quarks*, [*Phys. Rev.* **D 89** (2014) 014007](https://doi.org/) [[arXiv:1308.0540](https://arxiv.org/abs/1308.0540)] [INSPIRE].

The ATLAS collaboration

G. Aad[85], B. Abbott[113], J. Abdallah[151], O. Abdinov[11], R. Aben[107], M. Abolins[90],
O.S. AbouZeid[158], H. Abramowicz[153], H. Abreu[152], R. Abreu[116], Y. Abulaiti[146a,146b],
B.S. Acharya[164a,164b,a], L. Adamczyk[38a], D.L. Adams[25], J. Adelman[108], S. Adomeit[100],
T. Adye[131], A.A. Affolder[74], T. Agatonovic-Jovin[13], J. Agricola[54], J.A. Aguilar-Saavedra[126a,126f],
S.P. Ahlen[22], F. Ahmadov[65,b], G. Aielli[133a,133b], H. Akerstedt[146a,146b], T.P.A. Åkesson[81],
A.V. Akimov[96], G.L. Alberghi[20a,20b], J. Albert[169], S. Albrand[55], M.J. Alconada Verzini[71],
M. Aleksa[30], I.N. Aleksandrov[65], C. Alexa[26b], G. Alexander[153], T. Alexopoulos[10], M. Alhroob[113],
G. Alimonti[91a], L. Alio[85], J. Alison[31], S.P. Alkire[35], B.M.M. Allbrooke[149], P.P. Allport[18],
A. Aloisio[104a,104b], A. Alonso[36], F. Alonso[71], C. Alpigiani[138], A. Altheimer[35],
B. Alvarez Gonzalez[30], D. Álvarez Piqueras[167], M.G. Alviggi[104a,104b], B.T. Amadio[15],
K. Amako[66], Y. Amaral Coutinho[24a], C. Amelung[23], D. Amidei[89], S.P. Amor Dos Santos[126a,126c],
A. Amorim[126a,126b], S. Amoroso[48], N. Amram[153], G. Amundsen[23], C. Anastopoulos[139],
L.S. Ancu[49], N. Andari[108], T. Andeen[35], C.F. Anders[58b], G. Anders[30], J.K. Anders[74],
K.J. Anderson[31], A. Andreazza[91a,91b], V. Andrei[58a], S. Angelidakis[9], I. Angelozzi[107], P. Anger[44],
A. Angerami[35], F. Anghinolfi[30], A.V. Anisenkov[109,c], N. Anjos[12], A. Annovi[124a,124b],
M. Antonelli[47], A. Antonov[98], J. Antos[144b], F. Anulli[132a], M. Aoki[66], L. Aperio Bella[18],
G. Arabidze[90], Y. Arai[66], J.P. Araque[126a], A.T.H. Arce[45], F.A. Arduh[71], J-F. Arguin[95],
S. Argyropoulos[63], M. Arik[19a], A.J. Armbruster[30], O. Arnaez[30], H. Arnold[48], M. Arratia[28],
O. Arslan[21], A. Artamonov[97], G. Artoni[23], S. Artz[83], S. Asai[155], N. Asbah[42], A. Ashkenazi[153],
B. Åsman[146a,146b], L. Asquith[149], K. Assamagan[25], R. Astalos[144a], M. Atkinson[165], N.B. Atlay[141],
K. Augsten[128], M. Aurousseau[145b], G. Avolio[30], B. Axen[15], M.K. Ayoub[117], G. Azuelos[95,d],
M.A. Baak[30], A.E. Baas[58a], M.J. Baca[18], C. Bacci[134a,134b], H. Bachacou[136], K. Bachas[154],
M. Backes[30], M. Backhaus[30], P. Bagiacchi[132a,132b], P. Bagnaia[132a,132b], Y. Bai[33a], T. Bain[35],
J.T. Baines[131], O.K. Baker[176], E.M. Baldin[109,c], P. Balek[129], T. Balestri[148], F. Balli[84],
W.K. Balunas[122], E. Banas[39], Sw. Banerjee[173,e], A.A.E. Bannoura[175], L. Barak[30],
E.L. Barberio[88], D. Barberis[50a,50b], M. Barbero[85], T. Barillari[101], M. Barisonzi[164a,164b],
T. Barklow[143], N. Barlow[28], S.L. Barnes[84], B.M. Barnett[131], R.M. Barnett[15], Z. Barnovska[5],
A. Baroncelli[134a], G. Barone[23], A.J. Barr[120], F. Barreiro[82], J. Barreiro Guimarães da Costa[33a],
R. Bartoldus[143], A.E. Barton[72], P. Bartos[144a], A. Basalaev[123], A. Bassalat[117], A. Basye[165],
R.L. Bates[53], S.J. Batista[158], J.R. Batley[28], M. Battaglia[137], M. Bauce[132a,132b], F. Bauer[136],
H.S. Bawa[143,f], J.B. Beacham[111], M.D. Beattie[72], T. Beau[80], P.H. Beauchemin[161],
R. Beccherle[124a,124b], P. Bechtle[21], H.P. Beck[17,g], K. Becker[120], M. Becker[83], M. Beckingham[170],
C. Becot[117], A.J. Beddall[19b], A. Beddall[19b], V.A. Bednyakov[65], C.P. Bee[148], L.J. Beemster[107],
T.A. Beermann[30], M. Begel[25], J.K. Behr[120], C. Belanger-Champagne[87], W.H. Bell[49], G. Bella[153],
L. Bellagamba[20a], A. Bellerive[29], M. Bellomo[86], K. Belotskiy[98], O. Beltramello[30], O. Benary[153],
D. Benchekroun[135a], M. Bender[100], K. Bendtz[146a,146b], N. Benekos[10], Y. Benhammou[153],
E. Benhar Noccioli[49], J.A. Benitez Garcia[159b], D.P. Benjamin[45], J.R. Bensinger[23],
S. Bentvelsen[107], L. Beresford[120], M. Beretta[47], D. Berge[107], E. Bergeaas Kuutmann[166],
N. Berger[5], F. Berghaus[169], J. Beringer[15], C. Bernard[22], N.R. Bernard[86], C. Bernius[110],
F.U. Bernlochner[21], T. Berry[77], P. Berta[129], C. Bertella[83], G. Bertoli[146a,146b],
F. Bertolucci[124a,124b], C. Bertsche[113], D. Bertsche[113], M.I. Besana[91a], G.J. Besjes[36],
O. Bessidskaia Bylund[146a,146b], M. Bessner[42], N. Besson[136], C. Betancourt[48], S. Bethke[101],
A.J. Bevan[76], W. Bhimji[15], R.M. Bianchi[125], L. Bianchini[23], M. Bianco[30], O. Biebel[100],
D. Biedermann[16], N.V. Biesuz[124a,124b], M. Biglietti[134a], J. Bilbao De Mendizabal[49], H. Bilokon[47],
M. Bindi[54], S. Binet[117], A. Bingul[19b], C. Bini[132a,132b], S. Biondi[20a,20b], D.M. Bjergaard[45],
C.W. Black[150], J.E. Black[143], K.M. Black[22], D. Blackburn[138], R.E. Blair[6], J.-B. Blanchard[136],
J.E. Blanco[77], T. Blazek[144a], I. Bloch[42], C. Blocker[23], W. Blum[83,*], U. Blumenschein[54],
S. Blunier[32a], G.J. Bobbink[107], V.S. Bobrovnikov[109,c], S.S. Bocchetta[81], A. Bocci[45], C. Bock[100],
M. Boehler[48], J.A. Bogaerts[30], D. Bogavac[13], A.G. Bogdanchikov[109], C. Bohm[146a], V. Boisvert[77],
T. Bold[38a], V. Boldea[26b], A.S. Boldyrev[99], M. Bomben[80], M. Bona[76], M. Boonekamp[136],
A. Borisov[130], G. Borissov[72], S. Borroni[42], J. Bortfeldt[100], V. Bortolotto[60a,60b,60c], K. Bos[107],

D. Boscherini[20a], M. Bosman[12], J. Boudreau[125], J. Bouffard[2], E.V. Bouhova-Thacker[72],
D. Boumediene[34], C. Bourdarios[117], N. Bousson[114], S.K. Boutle[53], A. Boveia[30], J. Boyd[30],
I.R. Boyko[65], I. Bozic[13], J. Bracinik[18], A. Brandt[8], G. Brandt[54], O. Brandt[58a], U. Bratzler[156],
B. Brau[86], J.E. Brau[116], H.M. Braun[175,*], W.D. Breaden Madden[53], K. Brendlinger[122],
A.J. Brennan[88], L. Brenner[107], R. Brenner[166], S. Bressler[172], T.M. Bristow[46], D. Britton[53],
D. Britzger[42], F.M. Brochu[28], I. Brock[21], R. Brock[90], J. Bronner[101], G. Brooijmans[35],
T. Brooks[77], W.K. Brooks[32b], J. Brosamer[15], E. Brost[116], P.A. Bruckman de Renstrom[39],
D. Bruncko[144b], R. Bruneliere[48], A. Bruni[20a], G. Bruni[20a], M. Bruschi[20a], N. Bruscino[21],
L. Bryngemark[81], T. Buanes[14], Q. Buat[142], P. Buchholz[141], A.G. Buckley[53], I.A. Budagov[65],
F. Buehrer[48], L. Bugge[119], M.K. Bugge[119], O. Bulekov[98], D. Bullock[8], H. Burckhart[30],
S. Burdin[74], C.D. Burgard[48], B. Burghgrave[108], S. Burke[131], I. Burmeister[43], E. Busato[34],
D. Büscher[48], V. Büscher[83], P. Bussey[53], J.M. Butler[22], A.I. Butt[3], C.M. Buttar[53],
J.M. Butterworth[78], P. Butti[107], W. Buttinger[25], A. Buzatu[53], A.R. Buzykaev[109,c],
S. Cabrera Urbán[167], D. Caforio[128], V.M. Cairo[37a,37b], O. Cakir[4a], N. Calace[49], P. Calafiura[15],
A. Calandri[136], G. Calderini[80], P. Calfayan[100], L.P. Caloba[24a], D. Calvet[34], S. Calvet[34],
R. Camacho Toro[31], S. Camarda[42], P. Camarri[133a,133b], D. Cameron[119],
R. Caminal Armadans[165], S. Campana[30], M. Campanelli[78], A. Campoverde[148],
V. Canale[104a,104b], A. Canepa[159a], M. Cano Bret[33e], J. Cantero[82], R. Cantrill[126a], T. Cao[40],
M.D.M. Capeans Garrido[30], I. Caprini[26b], M. Caprini[26b], M. Capua[37a,37b], R. Caputo[83],
R.M. Carbone[35], R. Cardarelli[133a], F. Cardillo[48], T. Carli[30], G. Carlino[104a], L. Carminati[91a,91b],
S. Caron[106], E. Carquin[32a], G.D. Carrillo-Montoya[30], J.R. Carter[28], J. Carvalho[126a,126c],
D. Casadei[78], M.P. Casado[12], M. Casolino[12], D.W. Casper[163], E. Castaneda-Miranda[145a],
A. Castelli[107], V. Castillo Gimenez[167], N.F. Castro[126a,h], P. Catastini[57], A. Catinaccio[30],
J.R. Catmore[119], A. Cattai[30], J. Caudron[83], V. Cavaliere[165], D. Cavalli[91a], M. Cavalli-Sforza[12],
V. Cavasinni[124a,124b], F. Ceradini[134a,134b], L. Cerda Alberich[167], B.C. Cerio[45], K. Cerny[129],
A.S. Cerqueira[24b], A. Cerri[149], L. Cerrito[76], F. Cerutti[15], M. Cerv[30], A. Cervelli[17], S.A. Cetin[19c],
A. Chafaq[135a], D. Chakraborty[108], I. Chalupkova[129], Y.L. Chan[60a], P. Chang[165],
J.D. Chapman[28], D.G. Charlton[18], C.C. Chau[158], C.A. Chavez Barajas[149], S. Cheatham[152],
A. Chegwidden[90], S. Chekanov[6], S.V. Chekulaev[159a], G.A. Chelkov[65,i], M.A. Chelstowska[89],
C. Chen[64], H. Chen[25], K. Chen[148], L. Chen[33d,j], S. Chen[33c], S. Chen[155], X. Chen[33f], Y. Chen[67],
H.C. Cheng[89], Y. Cheng[31], A. Cheplakov[65], E. Cheremushkina[130], R. Cherkaoui El Moursli[135e],
V. Chernyatin[25,*], E. Cheu[7], L. Chevalier[136], V. Chiarella[47], G. Chiarelli[124a,124b], G. Chiodini[73a],
A.S. Chisholm[18], R.T. Chislett[78], A. Chitan[26b], M.V. Chizhov[65], K. Choi[61], S. Chouridou[9],
B.K.B. Chow[100], V. Christodoulou[78], D. Chromek-Burckhart[30], J. Chudoba[127], A.J. Chuinard[87],
J.J. Chwastowski[39], L. Chytka[115], G. Ciapetti[132a,132b], A.K. Ciftci[4a], D. Cinca[53], V. Cindro[75],
I.A. Cioara[21], A. Ciocio[15], F. Cirotto[104a,104b], Z.H. Citron[172], M. Ciubancan[26b], A. Clark[49],
B.L. Clark[57], P.J. Clark[46], R.N. Clarke[15], C. Clement[146a,146b], Y. Coadou[85], M. Cobal[164a,164c],
A. Coccaro[49], J. Cochran[64], L. Coffey[23], J.G. Cogan[143], L. Colasurdo[106], B. Cole[35], S. Cole[108],
A.P. Colijn[107], J. Collot[55], T. Colombo[58c], G. Compostella[101], P. Conde Muiño[126a,126b],
E. Coniavitis[48], S.H. Connell[145b], I.A. Connelly[77], V. Consorti[48], S. Constantinescu[26b],
C. Conta[121a,121b], G. Conti[30], F. Conventi[104a,k], M. Cooke[15], B.D. Cooper[78],
A.M. Cooper-Sarkar[120], T. Cornelissen[175], M. Corradi[20a], F. Corriveau[87,l], A. Corso-Radu[163],
A. Cortes-Gonzalez[12], G. Cortiana[101], G. Costa[91a], M.J. Costa[167], D. Costanzo[139], D. Côté[8],
G. Cottin[28], G. Cowan[77], B.E. Cox[84], K. Cranmer[110], G. Cree[29], S. Crépé-Renaudin[55],
F. Crescioli[80], W.A. Cribbs[146a,146b], M. Crispin Ortuzar[120], M. Cristinziani[21], V. Croft[106],
G. Crosetti[37a,37b], T. Cuhadar Donszelmann[139], J. Cummings[176], M. Curatolo[47], J. Cúth[83],
C. Cuthbert[150], H. Czirr[141], P. Czodrowski[3], S. D'Auria[53], M. D'Onofrio[74],
M.J. Da Cunha Sargedas De Sousa[126a,126b], C. Da Via[84], W. Dabrowski[38a], A. Dafinca[120],
T. Dai[89], O. Dale[14], F. Dallaire[95], C. Dallapiccola[86], M. Dam[36], J.R. Dandoy[31], N.P. Dang[48],
A.C. Daniells[18], M. Danninger[168], M. Dano Hoffmann[136], V. Dao[48], G. Darbo[50a], S. Darmora[8],
J. Dassoulas[3], A. Dattagupta[61], W. Davey[21], C. David[169], T. Davidek[129], E. Davies[120,m],
M. Davies[153], P. Davison[78], Y. Davygora[58a], E. Dawe[88], I. Dawson[139],

R.K. Daya-Ishmukhametova[86], K. De[8], R. de Asmundis[104a], A. De Benedetti[113],
S. De Castro[20a,20b], S. De Cecco[80], N. De Groot[106], P. de Jong[107], H. De la Torre[82],
F. De Lorenzi[64], D. De Pedis[132a], A. De Salvo[132a], U. De Sanctis[149], A. De Santo[149],
J.B. De Vivie De Regie[117], W.J. Dearnaley[72], R. Debbe[25], C. Debenedetti[137], D.V. Dedovich[65],
I. Deigaard[107], J. Del Peso[82], T. Del Prete[124a,124b], D. Delgove[117], F. Deliot[136], C.M. Delitzsch[49],
M. Deliyergiyev[75], A. Dell'Acqua[30], L. Dell'Asta[22], M. Dell'Orso[124a,124b], M. Della Pietra[104a,k],
D. della Volpe[49], M. Delmastro[5], P.A. Delsart[55], C. Deluca[107], D.A. DeMarco[158], S. Demers[176],
M. Demichev[65], A. Demilly[80], S.P. Denisov[130], D. Derendarz[39], J.E. Derkaoui[135d], F. Derue[80],
P. Dervan[74], K. Desch[21], C. Deterre[42], K. Dette[43], P.O. Deviveiros[30], A. Dewhurst[131],
S. Dhaliwal[23], A. Di Ciaccio[133a,133b], L. Di Ciaccio[5], A. Di Domenico[132a,132b],
C. Di Donato[104a,104b], A. Di Girolamo[30], B. Di Girolamo[30], A. Di Mattia[152], B. Di Micco[134a,134b],
R. Di Nardo[47], A. Di Simone[48], R. Di Sipio[158], D. Di Valentino[29], C. Diaconu[85], M. Diamond[158],
F.A. Dias[46], M.A. Diaz[32a], E.B. Diehl[89], J. Dietrich[16], S. Diglio[85], A. Dimitrievska[13],
J. Dingfelder[21], P. Dita[26b], S. Dita[26b], F. Dittus[30], F. Djama[85], T. Djobava[51b], J.I. Djuvsland[58a],
M.A.B. do Vale[24c], D. Dobos[30], M. Dobre[26b], C. Doglioni[81], T. Dohmae[155], J. Dolejsi[129],
Z. Dolezal[129], B.A. Dolgoshein[98,*], M. Donadelli[24d], S. Donati[124a,124b], P. Dondero[121a,121b],
J. Donini[34], J. Dopke[131], A. Doria[104a], M.T. Dova[71], A.T. Doyle[53], E. Drechsler[54], M. Dris[10],
Y. Du[33d], E. Dubreuil[34], E. Duchovni[172], G. Duckeck[100], O.A. Ducu[26b,85], D. Duda[107],
A. Dudarev[30], L. Duflot[117], L. Duguid[77], M. Dührssen[30], M. Dunford[58a], H. Duran Yildiz[4a],
M. Düren[52], A. Durglishvili[51b], D. Duschinger[44], B. Dutta[42], M. Dyndal[38a], C. Eckardt[42],
K.M. Ecker[101], R.C. Edgar[89], W. Edson[2], N.C. Edwards[46], W. Ehrenfeld[21], T. Eifert[30],
G. Eigen[14], K. Einsweiler[15], T. Ekelof[166], M. El Kacimi[135c], M. Ellert[166], S. Elles[5],
F. Ellinghaus[175], A.A. Elliot[169], N. Ellis[30], J. Elmsheuser[100], M. Elsing[30], D. Emeliyanov[131],
Y. Enari[155], O.C. Endner[83], M. Endo[118], J. Erdmann[43], A. Ereditato[17], G. Ernis[175], J. Ernst[2],
M. Ernst[25], S. Errede[165], E. Ertel[83], M. Escalier[117], H. Esch[43], C. Escobar[125], B. Esposito[47],
A.I. Etienvre[136], E. Etzion[153], H. Evans[61], A. Ezhilov[123], L. Fabbri[20a,20b], G. Facini[31],
R.M. Fakhrutdinov[130], S. Falciano[132a], R.J. Falla[78], J. Faltova[129], Y. Fang[33a], M. Fanti[91a,91b],
A. Farbin[8], A. Farilla[134a], T. Farooque[12], S. Farrell[15], S.M. Farrington[170], P. Farthouat[30],
F. Fassi[135e], P. Fassnacht[30], D. Fassouliotis[9], M. Faucci Giannelli[77], A. Favareto[50a,50b],
L. Fayard[117], O.L. Fedin[123,n], W. Fedorko[168], S. Feigl[30], L. Feligioni[85], C. Feng[33d], E.J. Feng[30],
H. Feng[89], A.B. Fenyuk[130], L. Feremenga[8], P. Fernandez Martinez[167], S. Fernandez Perez[30],
J. Ferrando[53], A. Ferrari[166], P. Ferrari[107], R. Ferrari[121a], D.E. Ferreira de Lima[53], A. Ferrer[167],
D. Ferrere[49], C. Ferretti[89], A. Ferretto Parodi[50a,50b], M. Fiascaris[31], F. Fiedler[83], A. Filipčič[75],
M. Filipuzzi[42], F. Filthaut[106], M. Fincke-Keeler[169], K.D. Finelli[150], M.C.N. Fiolhais[126a,126c],
L. Fiorini[167], A. Firan[40], A. Fischer[2], C. Fischer[12], J. Fischer[175], W.C. Fisher[90], N. Flaschel[42],
I. Fleck[141], P. Fleischmann[89], G.T. Fletcher[139], G. Fletcher[76], R.R.M. Fletcher[122], T. Flick[175],
A. Floderus[81], L.R. Flores Castillo[60a], M.J. Flowerdew[101], A. Formica[136], A. Forti[84],
D. Fournier[117], H. Fox[72], S. Fracchia[12], P. Francavilla[80], M. Franchini[20a,20b], D. Francis[30],
L. Franconi[119], M. Franklin[57], M. Frate[163], M. Fraternali[121a,121b], D. Freeborn[78], S.T. French[28],
S.M. Fressard-Batraneanu[30], F. Friedrich[44], D. Froidevaux[30], J.A. Frost[120], C. Fukunaga[156],
E. Fullana Torregrosa[83], B.G. Fulsom[143], T. Fusayasu[102], J. Fuster[167], C. Gabaldon[55],
O. Gabizon[175], A. Gabrielli[20a,20b], A. Gabrielli[15], G.P. Gach[18], S. Gadatsch[30], S. Gadomski[49],
G. Gagliardi[50a,50b], P. Gagnon[61], C. Galea[106], B. Galhardo[126a,126c], E.J. Gallas[120], B.J. Gallop[131],
P. Gallus[128], G. Galster[36], K.K. Gan[111], J. Gao[33b,85], Y. Gao[46], Y.S. Gao[143,f],
F.M. Garay Walls[46], F. Garberson[176], C. García[167], J.E. García Navarro[167], M. Garcia-Sciveres[15],
R.W. Gardner[31], N. Garelli[143], V. Garonne[119], C. Gatti[47], A. Gaudiello[50a,50b], G. Gaudio[121a],
B. Gaur[141], L. Gauthier[95], P. Gauzzi[132a,132b], I.L. Gavrilenko[96], C. Gay[168], G. Gaycken[21],
E.N. Gazis[10], P. Ge[33d], Z. Gecse[168], C.N.P. Gee[131], Ch. Geich-Gimbel[21], M.P. Geisler[58a],
C. Gemme[50a], M.H. Genest[55], C. Geng[33b,o], S. Gentile[132a,132b], M. George[54], S. George[77],
D. Gerbaudo[163], A. Gershon[153], S. Ghasemi[141], H. Ghazlane[135b], B. Giacobbe[20a],
S. Giagu[132a,132b], V. Giangiobbe[12], P. Giannetti[124a,124b], B. Gibbard[25], S.M. Gibson[77],
M. Gignac[168], M. Gilchriese[15], T.P.S. Gillam[28], D. Gillberg[30], G. Gilles[34], D.M. Gingrich[3,d],

N. Giokaris[9], M.P. Giordani[164a,164c], F.M. Giorgi[20a], F.M. Giorgi[16], P.F. Giraud[136],
P. Giromini[47], D. Giugni[91a], C. Giuliani[101], M. Giulini[58b], B.K. Gjelsten[119], S. Gkaitatzis[154],
I. Gkialas[154], E.L. Gkougkousis[117], L.K. Gladilin[99], C. Glasman[82], J. Glatzer[30],
P.C.F. Glaysher[46], A. Glazov[42], M. Goblirsch-Kolb[101], J.R. Goddard[76], J. Godlewski[39],
S. Goldfarb[89], T. Golling[49], D. Golubkov[130], A. Gomes[126a,126b,126d], R. Gonçalo[126a],
J. Goncalves Pinto Firmino Da Costa[136], L. Gonella[21], S. González de la Hoz[167],
G. Gonzalez Parra[12], S. Gonzalez-Sevilla[49], L. Goossens[30], P.A. Gorbounov[97], H.A. Gordon[25],
I. Gorelov[105], B. Gorini[30], E. Gorini[73a,73b], A. Gorišek[75], E. Gornicki[39], A.T. Goshaw[45],
C. Gössling[43], M.I. Gostkin[65], D. Goujdami[135c], A.G. Goussiou[138], N. Govender[145b],
E. Gozani[152], H.M.X. Grabas[137], L. Graber[54], I. Grabowska-Bold[38a], P.O.J. Gradin[166],
P. Grafström[20a,20b], J. Gramling[49], E. Gramstad[119], S. Grancagnolo[16], V. Gratchev[123],
H.M. Gray[30], E. Graziani[134a], Z.D. Greenwood[79,p], C. Grefe[21], K. Gregersen[78], I.M. Gregor[42],
P. Grenier[143], J. Griffiths[8], A.A. Grillo[137], K. Grimm[72], S. Grinstein[12,q], Ph. Gris[34],
J.-F. Grivaz[117], S. Groh[83], J.P. Grohs[44], A. Grohsjean[42], E. Gross[172], J. Grosse-Knetter[54],
G.C. Grossi[79], Z.J. Grout[149], L. Guan[89], J. Guenther[128], F. Guescini[49], D. Guest[163], O. Gueta[153],
E. Guido[50a,50b], T. Guillemin[117], S. Guindon[2], U. Gul[53], C. Gumpert[30], J. Guo[33e], Y. Guo[33b,o],
S. Gupta[120], G. Gustavino[132a,132b], P. Gutierrez[113], N.G. Gutierrez Ortiz[78], C. Gutschow[44],
C. Guyot[136], C. Gwenlan[120], C.B. Gwilliam[74], A. Haas[110], C. Haber[15], H.K. Hadavand[8],
N. Haddad[135e], P. Haefner[21], S. Hageböck[21], Z. Hajduk[39], H. Hakobyan[177], M. Haleem[42],
J. Haley[114], D. Hall[120], G. Halladjian[90], G.D. Hallewell[85], K. Hamacher[175], P. Hamal[115],
K. Hamano[169], A. Hamilton[145a], G.N. Hamity[139], P.G. Hamnett[42], L. Han[33b], K. Hanagaki[66,r],
K. Hanawa[155], M. Hance[137], B. Haney[122], P. Hanke[58a], R. Hanna[136], J.B. Hansen[36],
J.D. Hansen[36], M.C. Hansen[21], P.H. Hansen[36], K. Hara[160], A.S. Hard[173], T. Harenberg[175],
F. Hariri[117], S. Harkusha[92], R.D. Harrington[46], P.F. Harrison[170], F. Hartjes[107], M. Hasegawa[67],
Y. Hasegawa[140], A. Hasib[113], S. Hassani[136], S. Haug[17], R. Hauser[90], L. Hauswald[44],
M. Havranek[127], C.M. Hawkes[18], R.J. Hawkings[30], A.D. Hawkins[81], T. Hayashi[160], D. Hayden[90],
C.P. Hays[120], J.M. Hays[76], H.S. Hayward[74], S.J. Haywood[131], S.J. Head[18], T. Heck[83],
V. Hedberg[81], L. Heelan[8], S. Heim[122], T. Heim[175], B. Heinemann[15], L. Heinrich[110], J. Hejbal[127],
L. Helary[22], S. Hellman[146a,146b], C. Helsens[30], J. Henderson[120], R.C.W. Henderson[72], Y. Heng[173],
C. Hengler[42], S. Henkelmann[168], A. Henrichs[176], A.M. Henriques Correia[30], S. Henrot-Versille[117],
G.H. Herbert[16], Y. Hernández Jiménez[167], G. Herten[48], R. Hertenberger[100], L. Hervas[30],
G.G. Hesketh[78], N.P. Hessey[107], J.W. Hetherly[40], R. Hickling[76], E. Higón-Rodriguez[167],
E. Hill[169], J.C. Hill[28], K.H. Hiller[42], S.J. Hillier[18], I. Hinchliffe[15], E. Hines[122], R.R. Hinman[15],
M. Hirose[157], D. Hirschbuehl[175], J. Hobbs[148], N. Hod[107], M.C. Hodgkinson[139], P. Hodgson[139],
A. Hoecker[30], M.R. Hoeferkamp[105], F. Hoenig[100], M. Hohlfeld[83], D. Hohn[21], T.R. Holmes[15],
M. Homann[43], T.M. Hong[125], W.H. Hopkins[116], Y. Horii[103], A.J. Horton[142], J-Y. Hostachy[55],
S. Hou[151], A. Hoummada[135a], J. Howard[120], J. Howarth[42], M. Hrabovsky[115], I. Hristova[16],
J. Hrivnac[117], T. Hryn'ova[5], A. Hrynevich[93], C. Hsu[145c], P.J. Hsu[151,s], S.-C. Hsu[138], D. Hu[35],
Q. Hu[33b], X. Hu[89], Y. Huang[42], Z. Hubacek[128], F. Hubaut[85], F. Huegging[21], T.B. Huffman[120],
E.W. Hughes[35], G. Hughes[72], M. Huhtinen[30], T.A. Hülsing[83], N. Huseynov[65,b], J. Huston[90],
J. Huth[57], G. Iacobucci[49], G. Iakovidis[25], I. Ibragimov[141], L. Iconomidou-Fayard[117], E. Ideal[176],
Z. Idrissi[135e], P. Iengo[30], O. Igonkina[107], T. Iizawa[171], Y. Ikegami[66], K. Ikematsu[141], M. Ikeno[66],
Y. Ilchenko[31,t], D. Iliadis[154], N. Ilic[143], T. Ince[101], G. Introzzi[121a,121b], P. Ioannou[9], M. Iodice[134a],
K. Iordanidou[35], V. Ippolito[57], A. Irles Quiles[167], C. Isaksson[166], M. Ishino[68], M. Ishitsuka[157],
R. Ishmukhametov[111], C. Issever[120], S. Istin[19a], J.M. Iturbe Ponce[84], R. Iuppa[133a,133b],
J. Ivarsson[81], W. Iwanski[39], H. Iwasaki[66], J.M. Izen[41], V. Izzo[104a], S. Jabbar[3], B. Jackson[122],
M. Jackson[74], P. Jackson[1], M.R. Jaekel[30], V. Jain[2], K.B. Jakobi[83], K. Jakobs[48], S. Jakobsen[30],
T. Jakoubek[127], J. Jakubek[128], D.O. Jamin[114], D.K. Jana[79], E. Jansen[78], R. Jansky[62],
J. Janssen[21], M. Janus[54], G. Jarlskog[81], N. Javadov[65,b], T. Javůrek[48], L. Jeanty[15], J. Jejelava[51a,u],
G.-Y. Jeng[150], D. Jennens[88], P. Jenni[48,v], J. Jentzsch[43], C. Jeske[170], S. Jézéquel[5], H. Ji[173],
J. Jia[148], Y. Jiang[33b], S. Jiggins[78], J. Jimenez Pena[167], S. Jin[33a], A. Jinaru[26b], O. Jinnouchi[157],
M.D. Joergensen[36], P. Johansson[139], K.A. Johns[7], W.J. Johnson[138], K. Jon-And[146a,146b],

G. Jones[170], R.W.L. Jones[72], T.J. Jones[74], J. Jongmanns[58a], P.M. Jorge[126a,126b], K.D. Joshi[84],
J. Jovicevic[159a], X. Ju[173], A. Juste Rozas[12,q], M. Kaci[167], A. Kaczmarska[39], M. Kado[117],
H. Kagan[111], M. Kagan[143], S.J. Kahn[85], E. Kajomovitz[45], C.W. Kalderon[120], A. Kaluza[83],
S. Kama[40], A. Kamenshchikov[130], N. Kanaya[155], S. Kaneti[28], V.A. Kantserov[98], J. Kanzaki[66],
B. Kaplan[110], L.S. Kaplan[173], A. Kapliy[31], D. Kar[145c], K. Karakostas[10], A. Karamaoun[3],
N. Karastathis[10,107], M.J. Kareem[54], E. Karentzos[10], M. Karnevskiy[83], S.N. Karpov[65],
Z.M. Karpova[65], K. Karthik[110], V. Kartvelishvili[72], A.N. Karyukhin[130], K. Kasahara[160],
L. Kashif[173], R.D. Kass[111], A. Kastanas[14], Y. Kataoka[155], C. Kato[155], A. Katre[49], J. Katzy[42],
K. Kawade[103], K. Kawagoe[70], T. Kawamoto[155], G. Kawamura[54], S. Kazama[155],
V.F. Kazanin[109,c], R. Keeler[169], R. Kehoe[40], J.S. Keller[42], J.J. Kempster[77], H. Keoshkerian[84],
O. Kepka[127], B.P. Kerševan[75], S. Kersten[175], R.A. Keyes[87], F. Khalil-zada[11],
H. Khandanyan[146a,146b], A. Khanov[114], A.G. Kharlamov[109,c], T.J. Khoo[28], V. Khovanskiy[97],
E. Khramov[65], J. Khubua[51b,w], S. Kido[67], H.Y. Kim[8], S.H. Kim[160], Y.K. Kim[31], N. Kimura[154],
O.M. Kind[16], B.T. King[74], M. King[167], S.B. King[168], J. Kirk[131], A.E. Kiryunin[101],
T. Kishimoto[67], D. Kisielewska[38a], F. Kiss[48], K. Kiuchi[160], O. Kivernyk[136], E. Kladiva[144b],
M.H. Klein[35], M. Klein[74], U. Klein[74], K. Kleinknecht[83], P. Klimek[146a,146b], A. Klimentov[25],
R. Klingenberg[43], J.A. Klinger[139], T. Klioutchnikova[30], E.-E. Kluge[58a], P. Kluit[107], S. Kluth[101],
J. Knapik[39], E. Kneringer[62], E.B.F.G. Knoops[85], A. Knue[53], A. Kobayashi[155], D. Kobayashi[157],
T. Kobayashi[155], M. Kobel[44], M. Kocian[143], P. Kodys[129], T. Koffas[29], E. Koffeman[107],
L.A. Kogan[120], S. Kohlmann[175], Z. Kohout[128], T. Kohriki[66], T. Koi[143], H. Kolanoski[16],
M. Kolb[58b], I. Koletsou[5], A.A. Komar[96,*], Y. Komori[155], T. Kondo[66], N. Kondrashova[42],
K. Köneke[48], A.C. König[106], T. Kono[66], R. Konoplich[110,x], N. Konstantinidis[78],
R. Kopeliansky[152], S. Koperny[38a], L. Köpke[83], A.K. Kopp[48], K. Korcyl[39], K. Kordas[154],
A. Korn[78], A.A. Korol[109,c], I. Korolkov[12], E.V. Korolkova[139], O. Kortner[101], S. Kortner[101],
T. Kosek[129], V.V. Kostyukhin[21], V.M. Kotov[65], A. Kotwal[45], A. Kourkoumeli-Charalampidi[154],
C. Kourkoumelis[9], V. Kouskoura[25], A. Koutsman[159a], R. Kowalewski[169], T.Z. Kowalski[38a],
W. Kozanecki[136], A.S. Kozhin[130], V.A. Kramarenko[99], G. Kramberger[75], D. Krasnopevtsev[98],
M.W. Krasny[80], A. Krasznahorkay[30], J.K. Kraus[21], A. Kravchenko[25], S. Kreiss[110], M. Kretz[58c],
J. Kretzschmar[74], K. Kreutzfeldt[52], P. Krieger[158], K. Krizka[31], K. Kroeninger[43], H. Kroha[101],
J. Kroll[122], J. Kroseberg[21], J. Krstic[13], U. Kruchonak[65], H. Krüger[21], N. Krumnack[64],
A. Kruse[173], M.C. Kruse[45], M. Kruskal[22], T. Kubota[88], H. Kucuk[78], S. Kuday[4b], S. Kuehn[48],
A. Kugel[58c], F. Kuger[174], A. Kuhl[137], T. Kuhl[42], V. Kukhtin[65], R. Kukla[136], Y. Kulchitsky[92],
S. Kuleshov[32b], M. Kuna[132a,132b], T. Kunigo[68], A. Kupco[127], H. Kurashige[67], Y.A. Kurochkin[92],
V. Kus[127], E.S. Kuwertz[169], M. Kuze[157], J. Kvita[115], T. Kwan[169], D. Kyriazopoulos[139],
A. La Rosa[137], J.L. La Rosa Navarro[24d], L. La Rotonda[37a,37b], C. Lacasta[167], F. Lacava[132a,132b],
J. Lacey[29], H. Lacker[16], D. Lacour[80], V.R. Lacuesta[167], E. Ladygin[65], R. Lafaye[5], B. Laforge[80],
T. Lagouri[176], S. Lai[54], L. Lambourne[78], S. Lammers[61], C.L. Lampen[7], W. Lampl[7], E. Lançon[136],
U. Landgraf[48], M.P.J. Landon[76], V.S. Lang[58a], J.C. Lange[12], A.J. Lankford[163], F. Lanni[25],
K. Lantzsch[21], A. Lanza[121a], S. Laplace[80], C. Lapoire[30], J.F. Laporte[136], T. Lari[91a],
F. Lasagni Manghi[20a,20b], M. Lassnig[30], P. Laurelli[47], W. Lavrijsen[15], A.T. Law[137], P. Laycock[74],
T. Lazovich[57], O. Le Dortz[80], E. Le Guirriec[85], E. Le Menedeu[12], M. LeBlanc[169], T. LeCompte[6],
F. Ledroit-Guillon[55], C.A. Lee[145a], S.C. Lee[151], L. Lee[1], G. Lefebvre[80], M. Lefebvre[169],
F. Legger[100], C. Leggett[15], A. Lehan[74], G. Lehmann Miotto[30], X. Lei[7], W.A. Leight[29],
A. Leisos[154,y], A.G. Leister[176], M.A.L. Leite[24d], R. Leitner[129], D. Lellouch[172], B. Lemmer[54],
K.J.C. Leney[78], T. Lenz[21], B. Lenzi[30], R. Leone[7], S. Leone[124a,124b], C. Leonidopoulos[46],
S. Leontsinis[10], C. Leroy[95], C.G. Lester[28], M. Levchenko[123], J. Levêque[5], D. Levin[89],
L.J. Levinson[172], M. Levy[18], A. Lewis[120], A.M. Leyko[21], M. Leyton[41], B. Li[33b,z], H. Li[148],
H.L. Li[31], L. Li[45], L. Li[33e], S. Li[45], X. Li[84], Y. Li[33c,aa], Z. Liang[137], H. Liao[34], B. Liberti[133a],
A. Liblong[158], P. Lichard[30], K. Lie[165], J. Liebal[21], W. Liebig[14], C. Limbach[21], A. Limosani[150],
S.C. Lin[151,ab], T.H. Lin[83], F. Linde[107], B.E. Lindquist[148], J.T. Linnemann[90], E. Lipeles[122],
A. Lipniacka[14], M. Lisovyi[58b], T.M. Liss[165], D. Lissauer[25], A. Lister[168], A.M. Litke[137],
B. Liu[151,ac], D. Liu[151], H. Liu[89], J. Liu[85], J.B. Liu[33b], K. Liu[85], L. Liu[165], M. Liu[45], M. Liu[33b],

Y. Liu[33b], M. Livan[121a,121b], A. Lleres[55], J. Llorente Merino[82], S.L. Lloyd[76], F. Lo Sterzo[151],
E. Lobodzinska[42], P. Loch[7], W.S. Lockman[137], F.K. Loebinger[84], A.E. Loevschall-Jensen[36],
K.M. Loew[23], A. Loginov[176], T. Lohse[16], K. Lohwasser[42], M. Lokajicek[127], B.A. Long[22],
J.D. Long[165], R.E. Long[72], K.A. Looper[111], L. Lopes[126a], D. Lopez Mateos[57],
B. Lopez Paredes[139], I. Lopez Paz[12], J. Lorenz[100], N. Lorenzo Martinez[61], M. Losada[162],
P.J. Lösel[100], X. Lou[33a], A. Lounis[117], J. Love[6], P.A. Love[72], H. Lu[60a], N. Lu[89], H.J. Lubatti[138],
C. Luci[132a,132b], A. Lucotte[55], C. Luedtke[48], F. Luehring[61], W. Lukas[62], L. Luminari[132a],
O. Lundberg[146a,146b], B. Lund-Jensen[147], D. Lynn[25], R. Lysak[127], E. Lytken[81], H. Ma[25],
L.L. Ma[33d], G. Maccarrone[47], A. Macchiolo[101], C.M. Macdonald[139], B. Maček[75],
J. Machado Miguens[122,126b], D. Macina[30], D. Madaffari[85], R. Madar[34], H.J. Maddocks[72],
W.F. Mader[44], A. Madsen[166], J. Maeda[67], S. Maeland[14], T. Maeno[25], A. Maevskiy[99],
E. Magradze[54], K. Mahboubi[48], J. Mahlstedt[107], C. Maiani[136], C. Maidantchik[24a], A.A. Maier[101],
T. Maier[100], A. Maio[126a,126b,126d], S. Majewski[116], Y. Makida[66], N. Makovec[117], B. Malaescu[80],
Pa. Malecki[39], V.P. Maleev[123], F. Malek[55], U. Mallik[63], D. Malon[6], C. Malone[143], S. Maltezos[10],
V.M. Malyshev[109], S. Malyukov[30], J. Mamuzic[42], G. Mancini[47], B. Mandelli[30], L. Mandelli[91a],
I. Mandić[75], R. Mandrysch[63], J. Maneira[126a,126b], L. Manhaes de Andrade Filho[24b],
J. Manjarres Ramos[159b], A. Mann[100], A. Manousakis-Katsikakis[9], B. Mansoulie[136], R. Mantifel[87],
M. Mantoani[54], L. Mapelli[30], L. March[145c], G. Marchiori[80], M. Marcisovsky[127], C.P. Marino[169],
M. Marjanovic[13], D.E. Marley[89], F. Marroquim[24a], S.P. Marsden[84], Z. Marshall[15], L.F. Marti[17],
S. Marti-Garcia[167], B. Martin[90], T.A. Martin[170], V.J. Martin[46], B. Martin dit Latour[14],
M. Martinez[12,q], S. Martin-Haugh[131], V.S. Martoiu[26b], A.C. Martyniuk[78], M. Marx[138],
F. Marzano[132a], A. Marzin[30], L. Masetti[83], T. Mashimo[155], R. Mashinistov[96], J. Masik[84],
A.L. Maslennikov[109,c], I. Massa[20a,20b], L. Massa[20a,20b], P. Mastrandrea[5],
A. Mastroberardino[37a,37b], T. Masubuchi[155], P. Mättig[175], J. Mattmann[83], J. Maurer[26b],
S.J. Maxfield[74], D.A. Maximov[109,c], R. Mazini[151], S.M. Mazza[91a,91b], G. Mc Goldrick[158],
S.P. Mc Kee[89], A. McCarn[89], R.L. McCarthy[148], T.G. McCarthy[29], N.A. McCubbin[131],
K.W. McFarlane[56,*], J.A. Mcfayden[78], G. Mchedlidze[54], S.J. McMahon[131], R.A. McPherson[169,l],
M. Medinnis[42], S. Meehan[138], S. Mehlhase[100], A. Mehta[74], K. Meier[58a], C. Meineck[100],
B. Meirose[41], B.R. Mellado Garcia[145c], F. Meloni[17], A. Mengarelli[20a,20b], S. Menke[101],
E. Meoni[161], K.M. Mercurio[57], K. Meric[30], P. Mermod[49], L. Merola[104a,104b], C. Meroni[91a],
F.S. Merritt[31], A. Messina[132a,132b], J. Metcalfe[6], A.S. Mete[163], C. Meyer[83], C. Meyer[122],
J-P. Meyer[136], J. Meyer[107], H. Meyer Zu Theenhausen[58a], R.P. Middleton[131],
S. Miglioranzi[164a,164c], L. Mijović[21], G. Mikenberg[172], M. Mikestikova[127], M. Mikuž[75],
M. Milesi[88], A. Milic[30], D.W. Miller[31], C. Mills[46], A. Milov[172], D.A. Milstead[146a,146b],
A.A. Minaenko[130], Y. Minami[155], I.A. Minashvili[65], A.I. Mincer[110], B. Mindur[38a], M. Mineev[65],
Y. Ming[173], L.M. Mir[12], K.P. Mistry[122], T. Mitani[171], J. Mitrevski[100], V.A. Mitsou[167],
A. Miucci[49], P.S. Miyagawa[139], J.U. Mjörnmark[81], T. Moa[146a,146b], K. Mochizuki[85],
S. Mohapatra[35], W. Mohr[48], S. Molander[146a,146b], R. Moles-Valls[21], R. Monden[68],
M.C. Mondragon[90], K. Mönig[42], C. Monini[55], J. Monk[36], E. Monnier[85], A. Montalbano[148],
J. Montejo Berlingen[12], F. Monticelli[71], S. Monzani[132a,132b], R.W. Moore[3], N. Morange[117],
D. Moreno[162], M. Moreno Llácer[54], P. Morettini[50a], D. Mori[142], T. Mori[155], M. Morii[57],
M. Morinaga[155], V. Morisbak[119], S. Moritz[83], A.K. Morley[150], G. Mornacchi[30], J.D. Morris[76],
S.S. Mortensen[36], A. Morton[53], L. Morvaj[103], M. Mosidze[51b], J. Moss[143], K. Motohashi[157],
R. Mount[143], E. Mountricha[25], S.V. Mouraviev[96,*], E.J.W. Moyse[86], S. Muanza[85], R.D. Mudd[18],
F. Mueller[101], J. Mueller[125], R.S.P. Mueller[100], T. Mueller[28], D. Muenstermann[49], P. Mullen[53],
G.A. Mullier[17], F.J. Munoz Sanchez[84], J.A. Murillo Quijada[18], W.J. Murray[170,131],
H. Musheghyan[54], E. Musto[152], A.G. Myagkov[130,ad], M. Myska[128], B.P. Nachman[143],
O. Nackenhorst[54], J. Nadal[54], K. Nagai[120], R. Nagai[157], Y. Nagai[85], K. Nagano[66], A. Nagarkar[111],
Y. Nagasaka[59], K. Nagata[160], M. Nagel[101], E. Nagy[85], A.M. Nairz[30], Y. Nakahama[30],
K. Nakamura[66], T. Nakamura[155], I. Nakano[112], H. Namasivayam[41], R.F. Naranjo Garcia[42],
R. Narayan[31], D.I. Narrias Villar[58a], T. Naumann[42], G. Navarro[162], R. Nayyar[7], H.A. Neal[89],
P.Yu. Nechaeva[96], T.J. Neep[84], P.D. Nef[143], A. Negri[121a,121b], M. Negrini[20a], S. Nektarijevic[106],

C. Nellist[117], A. Nelson[163], S. Nemecek[127], P. Nemethy[110], A.A. Nepomuceno[24a], M. Nessi[30,ae],
M.S. Neubauer[165], M. Neumann[175], R.M. Neves[110], P. Nevski[25], P.R. Newman[18], D.H. Nguyen[6],
R.B. Nickerson[120], R. Nicolaidou[136], B. Nicquevert[30], J. Nielsen[137], N. Nikiforou[35], A. Nikiforov[16],
V. Nikolaenko[130,ad], I. Nikolic-Audit[80], K. Nikolopoulos[18], J.K. Nilsen[119], P. Nilsson[25],
Y. Ninomiya[155], A. Nisati[132a], R. Nisius[101], T. Nobe[155], M. Nomachi[118], I. Nomidis[29],
T. Nooney[76], S. Norberg[113], M. Nordberg[30], O. Novgorodova[44], S. Nowak[101], M. Nozaki[66],
L. Nozka[115], K. Ntekas[10], G. Nunes Hanninger[88], T. Nunnemann[100], E. Nurse[78], F. Nuti[88],
F. O'grady[7], D.C. O'Neil[142], V. O'Shea[53], F.G. Oakham[29,d], H. Oberlack[101], T. Obermann[21],
J. Ocariz[80], A. Ochi[67], I. Ochoa[35], J.P. Ochoa-Ricoux[32a], S. Oda[70], S. Odaka[66], H. Ogren[61],
A. Oh[84], S.H. Oh[45], C.C. Ohm[15], H. Ohman[166], H. Oide[30], W. Okamura[118], H. Okawa[160],
Y. Okumura[31], T. Okuyama[66], A. Olariu[26b], S.A. Olivares Pino[46], D. Oliveira Damazio[25],
A. Olszewski[39], J. Olszowska[39], A. Onofre[126a,126e], K. Onogi[103], P.U.E. Onyisi[31,t], C.J. Oram[159a],
M.J. Oreglia[31], Y. Oren[153], D. Orestano[134a,134b], N. Orlando[154], C. Oropeza Barrera[53],
R.S. Orr[158], B. Osculati[50a,50b], R. Ospanov[84], G. Otero y Garzon[27], H. Otono[70], M. Ouchrif[135d],
F. Ould-Saada[119], A. Ouraou[136], K.P. Oussoren[107], Q. Ouyang[33a], A. Ovcharova[15], M. Owen[53],
R.E. Owen[18], V.E. Ozcan[19a], N. Ozturk[8], K. Pachal[142], A. Pacheco Pages[12], C. Padilla Aranda[12],
M. Pagáčová[48], S. Pagan Griso[15], E. Paganis[139], F. Paige[25], P. Pais[86], K. Pajchel[119],
G. Palacino[159b], S. Palestini[30], M. Palka[38b], D. Pallin[34], A. Palma[126a,126b], Y.B. Pan[173],
E.St. Panagiotopoulou[10], C.E. Pandini[80], J.G. Panduro Vazquez[77], P. Pani[146a,146b], S. Panitkin[25],
D. Pantea[26b], L. Paolozzi[49], Th.D. Papadopoulou[10], K. Papageorgiou[154], A. Paramonov[6],
D. Paredes Hernandez[154], M.A. Parker[28], K.A. Parker[139], F. Parodi[50a,50b], J.A. Parsons[35],
U. Parzefall[48], E. Pasqualucci[132a], S. Passaggio[50a], F. Pastore[134a,134b,*], Fr. Pastore[77],
G. Pásztor[29], S. Pataraia[175], N.D. Patel[150], J.R. Pater[84], T. Pauly[30], J. Pearce[169], B. Pearson[113],
L.E. Pedersen[36], M. Pedersen[119], S. Pedraza Lopez[167], R. Pedro[126a,126b], S.V. Peleganchuk[109,c],
D. Pelikan[166], O. Penc[127], C. Peng[33a], H. Peng[33b], B. Penning[31], J. Penwell[61], D.V. Perepelitsa[25],
E. Perez Codina[159a], M.T. Pérez García-Estañ[167], L. Perini[91a,91b], H. Pernegger[30],
S. Perrella[104a,104b], R. Peschke[42], V.D. Peshekhonov[65], K. Peters[30], R.F.Y. Peters[84],
B.A. Petersen[30], T.C. Petersen[36], E. Petit[42], A. Petridis[1], C. Petridou[154], P. Petroff[117],
E. Petrolo[132a], F. Petrucci[134a,134b], N.E. Pettersson[157], R. Pezoa[32b], P.W. Phillips[131],
G. Piacquadio[143], E. Pianori[170], A. Picazio[49], E. Piccaro[76], M. Piccinini[20a,20b], M.A. Pickering[120],
R. Piegaia[27], D.T. Pignotti[111], J.E. Pilcher[31], A.D. Pilkington[84], A.W.J. Pin[84],
J. Pina[126a,126b,126d], M. Pinamonti[164a,164c,af], J.L. Pinfold[3], A. Pingel[36], S. Pires[80],
H. Pirumov[42], M. Pitt[172], C. Pizio[91a,91b], L. Plazak[144a], M.-A. Pleier[25], V. Pleskot[129],
E. Plotnikova[65], P. Plucinski[146a,146b], D. Pluth[64], R. Poettgen[146a,146b], L. Poggioli[117], D. Pohl[21],
G. Polesello[121a], A. Poley[42], A. Policicchio[37a,37b], R. Polifka[158], A. Polini[20a], C.S. Pollard[53],
V. Polychronakos[25], K. Pommès[30], L. Pontecorvo[132a], B.G. Pope[90], G.A. Popeneciu[26c],
D.S. Popovic[13], A. Poppleton[30], S. Pospisil[128], K. Potamianos[15], I.N. Potrap[65], C.J. Potter[149],
C.T. Potter[116], G. Poulard[30], J. Poveda[30], V. Pozdnyakov[65], M.E. Pozo Astigarraga[30],
P. Pralavorio[85], A. Pranko[15], S. Prasad[30], S. Prell[64], D. Price[84], L.E. Price[6], M. Primavera[73a],
S. Prince[87], M. Proissl[46], K. Prokofiev[60c], F. Prokoshin[32b], E. Protopapadaki[136],
S. Protopopescu[25], J. Proudfoot[6], M. Przybycien[38a], E. Ptacek[116], D. Puddu[134a,134b],
E. Pueschel[86], D. Puldon[148], M. Purohit[25,ag], P. Puzo[117], J. Qian[89], G. Qin[53], Y. Qin[84],
A. Quadt[54], D.R. Quarrie[15], W.B. Quayle[164a,164b], M. Queitsch-Maitland[84], D. Quilty[53],
S. Raddum[119], V. Radeka[25], V. Radescu[42], S.K. Radhakrishnan[148], P. Radloff[116], P. Rados[88],
F. Ragusa[91a,91b], G. Rahal[178], S. Rajagopalan[25], M. Rammensee[30], C. Rangel-Smith[166],
F. Rauscher[100], S. Rave[83], T. Ravenscroft[53], M. Raymond[30], A.L. Read[119], N.P. Readioff[74],
D.M. Rebuzzi[121a,121b], A. Redelbach[174], G. Redlinger[25], R. Reece[137], K. Reeves[41], L. Rehnisch[16],
J. Reichert[122], H. Reisin[27], C. Rembser[30], H. Ren[33a], A. Renaud[117], M. Rescigno[132a],
S. Resconi[91a], O.L. Rezanova[109,c], P. Reznicek[129], R. Rezvani[95], R. Richter[101], S. Richter[78],
E. Richter-Was[38b], O. Ricken[21], M. Ridel[80], P. Rieck[16], C.J. Riegel[175], J. Rieger[54], O. Rifki[113],
M. Rijssenbeek[148], A. Rimoldi[121a,121b], L. Rinaldi[20a], B. Ristić[49], E. Ritsch[30], I. Riu[12],
F. Rizatdinova[114], E. Rizvi[76], S.H. Robertson[87,l], A. Robichaud-Veronneau[87], D. Robinson[28],

J.E.M. Robinson[42], A. Robson[53], C. Roda[124a,124b], S. Roe[30], O. Røhne[119], A. Romaniouk[98], M. Romano[20a,20b], S.M. Romano Saez[34], E. Romero Adam[167], N. Rompotis[138], M. Ronzani[48], L. Roos[80], E. Ros[167], S. Rosati[132a], K. Rosbach[48], P. Rose[137], O. Rosenthal[141], V. Rossetti[146a,146b], E. Rossi[104a,104b], L.P. Rossi[50a], J.H.N. Rosten[28], R. Rosten[138], M. Rotaru[26b], I. Roth[172], J. Rothberg[138], D. Rousseau[117], C.R. Royon[136], A. Rozanov[85], Y. Rozen[152], X. Ruan[145c], F. Rubbo[143], I. Rubinskiy[42], V.I. Rud[99], C. Rudolph[44], M.S. Rudolph[158], F. Rühr[48], A. Ruiz-Martinez[30], Z. Rurikova[48], N.A. Rusakovich[65], A. Ruschke[100], H.L. Russell[138], J.P. Rutherfoord[7], N. Ruthmann[30], Y.F. Ryabov[123], M. Rybar[165], G. Rybkin[117], N.C. Ryder[120], A.F. Saavedra[150], G. Sabato[107], S. Sacerdoti[27], A. Saddique[3], H.F-W. Sadrozinski[137], R. Sadykov[65], F. Safai Tehrani[132a], P. Saha[108], M. Sahinsoy[58a], M. Saimpert[136], T. Saito[155], H. Sakamoto[155], Y. Sakurai[171], G. Salamanna[134a,134b], A. Salamon[133a], J.E. Salazar Loyola[32b], M. Saleem[113], D. Salek[107], P.H. Sales De Bruin[138], D. Salihagic[101], A. Salnikov[143], J. Salt[167], D. Salvatore[37a,37b], F. Salvatore[149], A. Salvucci[60a], A. Salzburger[30], D. Sammel[48], D. Sampsonidis[154], A. Sanchez[104a,104b], J. Sánchez[167], V. Sanchez Martinez[167], H. Sandaker[119], R.L. Sandbach[76], H.G. Sander[83], M.P. Sanders[100], M. Sandhoff[175], C. Sandoval[162], R. Sandstroem[101], D.P.C. Sankey[131], M. Sannino[50a,50b], A. Sansoni[47], C. Santoni[34], R. Santonico[133a,133b], H. Santos[126a], I. Santoyo Castillo[149], K. Sapp[125], A. Sapronov[65], J.G. Saraiva[126a,126d], B. Sarrazin[21], O. Sasaki[66], Y. Sasaki[155], K. Sato[160], G. Sauvage[5,*], E. Sauvan[5], G. Savage[77], P. Savard[158,d], C. Sawyer[131], L. Sawyer[79,p], J. Saxon[31], C. Sbarra[20a], A. Sbrizzi[20a,20b], T. Scanlon[78], D.A. Scannicchio[163], M. Scarcella[150], V. Scarfone[37a,37b], J. Schaarschmidt[172], P. Schacht[101], D. Schaefer[30], R. Schaefer[42], J. Schaeffer[83], S. Schaepe[21], S. Schaetzel[58b], U. Schäfer[83], A.C. Schaffer[117], D. Schaile[100], R.D. Schamberger[148], V. Scharf[58a], V.A. Schegelsky[123], D. Scheirich[129], M. Schernau[163], C. Schiavi[50a,50b], C. Schillo[48], M. Schioppa[37a,37b], S. Schlenker[30], K. Schmieden[30], C. Schmitt[83], S. Schmitt[58b], S. Schmitt[42], S. Schmitz[83], B. Schneider[159a], Y.J. Schnellbach[74], U. Schnoor[44], L. Schoeffel[136], A. Schoening[58b], B.D. Schoenrock[90], E. Schopf[21], A.L.S. Schorlemmer[54], M. Schott[83], D. Schouten[159a], J. Schovancova[8], S. Schramm[49], M. Schreyer[174], N. Schuh[83], M.J. Schultens[21], H.-C. Schultz-Coulon[58a], H. Schulz[16], M. Schumacher[48], B.A. Schumm[137], Ph. Schune[136], C. Schwanenberger[84], A. Schwartzman[143], T.A. Schwarz[89], Ph. Schwegler[101], H. Schweiger[84], Ph. Schwemling[136], R. Schwienhorst[90], J. Schwindling[136], T. Schwindt[21], F.G. Sciacca[17], E. Scifo[117], G. Sciolla[23], F. Scuri[124a,124b], F. Scutti[21], J. Searcy[89], G. Sedov[42], E. Sedykh[123], P. Seema[21], S.C. Seidel[105], A. Seiden[137], F. Seifert[128], J.M. Seixas[24a], G. Sekhniaidze[104a], K. Sekhon[89], S.J. Sekula[40], D.M. Seliverstov[123,*], N. Semprini-Cesari[20a,20b], C. Serfon[30], L. Serin[117], L. Serkin[164a,164b], T. Serre[85], M. Sessa[134a,134b], R. Seuster[159a], H. Severini[113], T. Sfiligoj[75], F. Sforza[30], A. Sfyrla[30], E. Shabalina[54], M. Shamim[116], L.Y. Shan[33a], R. Shang[165], J.T. Shank[22], M. Shapiro[15], P.B. Shatalov[97], K. Shaw[164a,164b], S.M. Shaw[84], A. Shcherbakova[146a,146b], C.Y. Shehu[149], P. Sherwood[78], L. Shi[151,ah], S. Shimizu[67], C.O. Shimmin[163], M. Shimojima[102], M. Shiyakova[65], A. Shmeleva[96], D. Shoaleh Saadi[95], M.J. Shochet[31], S. Shojaii[91a,91b], S. Shrestha[111], E. Shulga[98], M.A. Shupe[7], P. Sicho[127], P.E. Sidebo[147], O. Sidiropoulou[174], D. Sidorov[114], A. Sidoti[20a,20b], F. Siegert[44], Dj. Sijacki[13], J. Silva[126a,126d], Y. Silver[153], S.B. Silverstein[146a], V. Simak[128], O. Simard[5], Lj. Simic[13], S. Simion[117], E. Simioni[83], B. Simmons[78], D. Simon[34], M. Simon[83], P. Sinervo[158], N.B. Sinev[116], M. Sioli[20a,20b], G. Siragusa[174], A.N. Sisakyan[65,*], S.Yu. Sivoklokov[99], J. Sjölin[146a,146b], T.B. Sjursen[14], M.B. Skinner[72], H.P. Skottowe[57], P. Skubic[113], M. Slater[18], T. Slavicek[128], M. Slawinska[107], K. Sliwa[161], V. Smakhtin[172], B.H. Smart[46], L. Smestad[14], S.Yu. Smirnov[98], Y. Smirnov[98], L.N. Smirnova[99,ai], O. Smirnova[81], M.N.K. Smith[35], R.W. Smith[35], M. Smizanska[72], K. Smolek[128], A.A. Snesarev[96], G. Snidero[76], S. Snyder[25], R. Sobie[169,l], F. Socher[44], A. Soffer[153], D.A. Soh[151,ah], G. Sokhrannyi[75], C.A. Solans[30], M. Solar[128], J. Solc[128], E.Yu. Soldatov[98], U. Soldevila[167], A.A. Solodkov[130], A. Soloshenko[65], O.V. Solovyanov[130], V. Solovyev[123], P. Sommer[48], H.Y. Song[33b,z], N. Soni[1], A. Sood[15], A. Sopczak[128], B. Sopko[128], V. Sopko[128], V. Sorin[12], D. Sosa[58b], M. Sosebee[8], C.L. Sotiropoulou[124a,124b], R. Soualah[164a,164c], A.M. Soukharev[109,c], D. South[42], B.C. Sowden[77], S. Spagnolo[73a,73b], M. Spalla[124a,124b],

M. Spangenberg[170], F. Spanò[77], W.R. Spearman[57], D. Sperlich[16], F. Spettel[101], R. Spighi[20a],
G. Spigo[30], L.A. Spiller[88], M. Spousta[129], R.D. St. Denis[53,*], A. Stabile[91a], S. Staerz[30],
J. Stahlman[122], R. Stamen[58a], S. Stamm[16], E. Stanecka[39], C. Stanescu[134a], M. Stanescu-Bellu[42],
M.M. Stanitzki[42], S. Stapnes[119], E.A. Starchenko[130], J. Stark[55], P. Staroba[127], P. Starovoitov[58a],
R. Staszewski[39], P. Steinberg[25], B. Stelzer[142], H.J. Stelzer[30], O. Stelzer-Chilton[159a], H. Stenzel[52],
G.A. Stewart[53], J.A. Stillings[21], M.C. Stockton[87], M. Stoebe[87], G. Stoicea[26b], P. Stolte[54],
S. Stonjek[101], A.R. Stradling[8], A. Straessner[44], M.E. Stramaglia[17], J. Strandberg[147],
S. Strandberg[146a,146b], A. Strandlie[119], E. Strauss[143], M. Strauss[113], P. Strizenec[144b],
R. Ströhmer[174], D.M. Strom[116], R. Stroynowski[40], A. Strubig[106], S.A. Stucci[17], B. Stugu[14],
N.A. Styles[42], D. Su[143], J. Su[125], R. Subramaniam[79], A. Succurro[12], S. Suchek[58a], Y. Sugaya[118],
M. Suk[128], V.V. Sulin[96], S. Sultansoy[4c], T. Sumida[68], S. Sun[57], X. Sun[33a], J.E. Sundermann[48],
K. Suruliz[149], G. Susinno[37a,37b], M.R. Sutton[149], S. Suzuki[66], M. Svatos[127], M. Swiatlowski[31],
I. Sykora[144a], T. Sykora[129], D. Ta[48], C. Taccini[134a,134b], K. Tackmann[42], J. Taenzer[158],
A. Taffard[163], R. Tafirout[159a], N. Taiblum[153], H. Takai[25], R. Takashima[69], H. Takeda[67],
T. Takeshita[140], Y. Takubo[66], M. Talby[85], A.A. Talyshev[109,c], J.Y.C. Tam[174], K.G. Tan[88],
J. Tanaka[155], R. Tanaka[117], S. Tanaka[66], B.B. Tannenwald[111], S. Tapia Araya[32b], S. Tapprogge[83],
S. Tarem[152], F. Tarrade[29], G.F. Tartarelli[91a], P. Tas[129], M. Tasevsky[127], T. Tashiro[68],
E. Tassi[37a,37b], A. Tavares Delgado[126a,126b], Y. Tayalati[135d], A.C. Taylor[105], F.E. Taylor[94],
G.N. Taylor[88], P.T.E. Taylor[88], W. Taylor[159b], F.A. Teischinger[30],
M. Teixeira Dias Castanheira[76], P. Teixeira-Dias[77], K.K. Temming[48], D. Temple[142],
H. Ten Kate[30], P.K. Teng[151], J.J. Teoh[118], F. Tepel[175], S. Terada[66], K. Terashi[155], J. Terron[82],
S. Terzo[101], M. Testa[47], R.J. Teuscher[158,l], T. Theveneaux-Pelzer[34], J.P. Thomas[18],
J. Thomas-Wilsker[77], E.N. Thompson[35], P.D. Thompson[18], R.J. Thompson[84], A.S. Thompson[53],
L.A. Thomsen[176], E. Thomson[122], M. Thomson[28], R.P. Thun[89,*], M.J. Tibbetts[15],
R.E. Ticse Torres[85], V.O. Tikhomirov[96,aj], Yu.A. Tikhonov[109,c], S. Timoshenko[98],
E. Tiouchichine[85], P. Tipton[176], S. Tisserant[85], K. Todome[157], T. Todorov[5,*],
S. Todorova-Nova[129], J. Tojo[70], S. Tokár[144a], K. Tokushuku[66], K. Tollefson[90], E. Tolley[57],
L. Tomlinson[84], M. Tomoto[103], L. Tompkins[143,ak], K. Toms[105], E. Torrence[116], H. Torres[142],
E. Torró Pastor[138], J. Toth[85,al], F. Touchard[85], D.R. Tovey[139], T. Trefzger[174], L. Tremblet[30],
A. Tricoli[30], I.M. Trigger[159a], S. Trincaz-Duvoid[80], M.F. Tripiana[12], W. Trischuk[158], B. Trocmé[55],
C. Troncon[91a], M. Trottier-McDonald[15], M. Trovatelli[169], L. Truong[164a,164c], M. Trzebinski[39],
A. Trzupek[39], C. Tsarouchas[30], J.C-L. Tseng[120], P.V. Tsiareshka[92], D. Tsionou[154],
G. Tsipolitis[10], N. Tsirintanis[9], S. Tsiskaridze[12], V. Tsiskaridze[48], E.G. Tskhadadze[51a],
K.M. Tsui[60a], I.I. Tsukerman[97], V. Tsulaia[15], S. Tsuno[66], D. Tsybychev[148], A. Tudorache[26b],
V. Tudorache[26b], A.N. Tuna[57], S.A. Tupputi[20a,20b], S. Turchikhin[99,ai], D. Turecek[128],
R. Turra[91a,91b], A.J. Turvey[40], P.M. Tuts[35], A. Tykhonov[49], M. Tylmad[146a,146b], M. Tyndel[131],
I. Ueda[155], R. Ueno[29], M. Ughetto[146a,146b], F. Ukegawa[160], G. Unal[30], A. Undrus[25], G. Unel[163],
F.C. Ungaro[88], Y. Unno[66], C. Unverdorben[100], J. Urban[144b], P. Urquijo[88], P. Urrejola[83],
G. Usai[8], A. Usanova[62], L. Vacavant[85], V. Vacek[128], B. Vachon[87], C. Valderanis[83], N. Valencic[107],
S. Valentinetti[20a,20b], A. Valero[167], L. Valery[12], S. Valkar[129], S. Vallecorsa[49], J.A. Valls Ferrer[167],
W. Van Den Wollenberg[107], P.C. Van Der Deijl[107], R. van der Geer[107], H. van der Graaf[107],
N. van Eldik[152], P. van Gemmeren[6], J. Van Nieuwkoop[142], I. van Vulpen[107], M.C. van Woerden[30],
M. Vanadia[132a,132b], W. Vandelli[30], R. Vanguri[122], A. Vaniachine[6], F. Vannucci[80],
G. Vardanyan[177], R. Vari[132a], E.W. Varnes[7], T. Varol[40], D. Varouchas[80], A. Vartapetian[8],
K.E. Varvell[150], F. Vazeille[34], T. Vazquez Schroeder[87], J. Veatch[7], L.M. Veloce[158],
F. Veloso[126a,126c], T. Velz[21], S. Veneziano[132a], A. Ventura[73a,73b], D. Ventura[86], M. Venturi[169],
N. Venturi[158], A. Venturini[23], V. Vercesi[121a], M. Verducci[132a,132b], W. Verkerke[107],
J.C. Vermeulen[107], A. Vest[44], M.C. Vetterli[142,d], O. Viazlo[81], I. Vichou[165], T. Vickey[139],
O.E. Vickey Boeriu[139], G.H.A. Viehhauser[120], S. Viel[15], R. Vigne[62], M. Villa[20a,20b],
M. Villaplana Perez[91a,91b], E. Vilucchi[47], M.G. Vincter[29], V.B. Vinogradov[65], I. Vivarelli[149],
S. Vlachos[10], D. Vladoiu[100], M. Vlasak[128], M. Vogel[32a], P. Vokac[128], G. Volpi[124a,124b], M. Volpi[88],
H. von der Schmitt[101], H. von Radziewski[48], E. von Toerne[21], V. Vorobel[129], K. Vorobev[98],

M. Vos[167], R. Voss[30], J.H. Vossebeld[74], N. Vranjes[13], M. Vranjes Milosavljevic[13], V. Vrba[127], M. Vreeswijk[107], R. Vuillermet[30], I. Vukotic[31], Z. Vykydal[128], P. Wagner[21], W. Wagner[175], H. Wahlberg[71], S. Wahrmund[44], J. Wakabayashi[103], J. Walder[72], R. Walker[100], W. Walkowiak[141], C. Wang[151], F. Wang[173], H. Wang[15], H. Wang[40], J. Wang[42], J. Wang[150], K. Wang[87], R. Wang[6], S.M. Wang[151], T. Wang[21], T. Wang[35], X. Wang[176], C. Wanotayaroj[116], A. Warburton[87], C.P. Ward[28], D.R. Wardrope[78], A. Washbrook[46], C. Wasicki[42], P.M. Watkins[18], A.T. Watson[18], I.J. Watson[150], M.F. Watson[18], G. Watts[138], S. Watts[84], B.M. Waugh[78], S. Webb[84], M.S. Weber[17], S.W. Weber[174], J.S. Webster[6], A.R. Weidberg[120], B. Weinert[61], J. Weingarten[54], C. Weiser[48], H. Weits[107], P.S. Wells[30], T. Wenaus[25], T. Wengler[30], S. Wenig[30], N. Wermes[21], M. Werner[48], P. Werner[30], M. Wessels[58a], J. Wetter[161], K. Whalen[116], A.M. Wharton[72], A. White[8], M.J. White[1], R. White[32b], S. White[124a,124b], D. Whiteson[163], F.J. Wickens[131], W. Wiedenmann[173], M. Wielers[131], P. Wienemann[21], C. Wiglesworth[36], L.A.M. Wiik-Fuchs[21], A. Wildauer[101], H.G. Wilkens[30], H.H. Williams[122], S. Williams[107], C. Willis[90], S. Willocq[86], A. Wilson[89], J.A. Wilson[18], I. Wingerter-Seez[5], F. Winklmeier[116], B.T. Winter[21], M. Wittgen[143], J. Wittkowski[100], S.J. Wollstadt[83], M.W. Wolter[39], H. Wolters[126a,126c], B.K. Wosiek[39], J. Wotschack[30], M.J. Woudstra[84], K.W. Wozniak[39], M. Wu[55], M. Wu[31], S.L. Wu[173], X. Wu[49], Y. Wu[89], T.R. Wyatt[84], B.M. Wynne[46], S. Xella[36], D. Xu[33a], L. Xu[25], B. Yabsley[150], S. Yacoob[145a], R. Yakabe[67], M. Yamada[66], D. Yamaguchi[157], Y. Yamaguchi[118], A. Yamamoto[66], S. Yamamoto[155], T. Yamanaka[155], K. Yamauchi[103], Y. Yamazaki[67], Z. Yan[22], H. Yang[33e], H. Yang[173], Y. Yang[151], W-M. Yao[15], Y.C. Yap[80], Y. Yasu[66], E. Yatsenko[5], K.H. Yau Wong[21], J. Ye[40], S. Ye[25], I. Yeletskikh[65], A.L. Yen[57], E. Yildirim[42], K. Yorita[171], R. Yoshida[6], K. Yoshihara[122], C. Young[143], C.J.S. Young[30], S. Youssef[22], D.R. Yu[15], J. Yu[8], J.M. Yu[89], J. Yu[114], L. Yuan[67], S.P.Y. Yuen[21], A. Yurkewicz[108], I. Yusuff[28,am], B. Zabinski[39], R. Zaidan[63], A.M. Zaitsev[130,ad], J. Zalieckas[14], A. Zaman[148], S. Zambito[57], L. Zanello[132a,132b], D. Zanzi[88], C. Zeitnitz[175], M. Zeman[128], A. Zemla[38a], J.C. Zeng[165], Q. Zeng[143], K. Zengel[23], O. Zenin[130], T. Ženiš[144a], D. Zerwas[117], D. Zhang[89], F. Zhang[173], G. Zhang[33b], H. Zhang[33c], J. Zhang[6], L. Zhang[48], R. Zhang[33b,j], X. Zhang[33d], Z. Zhang[117], X. Zhao[40], Y. Zhao[33d,117], Z. Zhao[33b], A. Zhemchugov[65], J. Zhong[120], B. Zhou[89], C. Zhou[45], L. Zhou[35], L. Zhou[40], M. Zhou[148], N. Zhou[33f], C.G. Zhu[33d], H. Zhu[33a], J. Zhu[89], Y. Zhu[33b], X. Zhuang[33a], K. Zhukov[96], A. Zibell[174], D. Zieminska[61], N.I. Zimine[65], C. Zimmermann[83], S. Zimmermann[48], Z. Zinonos[54], M. Zinser[83], M. Ziolkowski[141], L. Živković[13], G. Zobernig[173], A. Zoccoli[20a,20b], M. zur Nedden[16], G. Zurzolo[104a,104b], L. Zwalinski[30]

1   Department of Physics, University of Adelaide, Adelaide, Australia
2   Physics Department, SUNY Albany, Albany NY, United States of America
3   Department of Physics, University of Alberta, Edmonton AB, Canada
4   (a) Department of Physics, Ankara University, Ankara; (b) Istanbul Aydin University, Istanbul; (c) Division of Physics, TOBB University of Economics and Technology, Ankara, Turkey
5   LAPP, CNRS/IN2P3 and Université Savoie Mont Blanc, Annecy-le-Vieux, France
6   High Energy Physics Division, Argonne National Laboratory, Argonne IL, United States of America
7   Department of Physics, University of Arizona, Tucson AZ, United States of America
8   Department of Physics, The University of Texas at Arlington, Arlington TX, United States of America
9   Physics Department, University of Athens, Athens, Greece
10   Physics Department, National Technical University of Athens, Zografou, Greece
11   Institute of Physics, Azerbaijan Academy of Sciences, Baku, Azerbaijan
12   Institut de Física d'Altes Energies and Departament de Física de la Universitat Autònoma de Barcelona, Barcelona, Spain
13   Institute of Physics, University of Belgrade, Belgrade, Serbia
14   Department for Physics and Technology, University of Bergen, Bergen, Norway
15   Physics Division, Lawrence Berkeley National Laboratory and University of California, Berkeley CA, United States of America
16   Department of Physics, Humboldt University, Berlin, Germany

17 Albert Einstein Center for Fundamental Physics and Laboratory for High Energy Physics, University of Bern, Bern, Switzerland

18 School of Physics and Astronomy, University of Birmingham, Birmingham, United Kingdom

19 [a] Department of Physics, Bogazici University, Istanbul; [b] Department of Physics Engineering, Gaziantep University, Gaziantep; [c] Department of Physics, Dogus University, Istanbul, Turkey

20 [a] INFN Sezione di Bologna; [b] Dipartimento di Fisica e Astronomia, Università di Bologna, Bologna, Italy

21 Physikalisches Institut, University of Bonn, Bonn, Germany

22 Department of Physics, Boston University, Boston MA, United States of America

23 Department of Physics, Brandeis University, Waltham MA, United States of America

24 [a] Universidade Federal do Rio De Janeiro COPPE/EE/IF, Rio de Janeiro; [b] Electrical Circuits Department, Federal University of Juiz de Fora (UFJF), Juiz de Fora; [c] Federal University of Sao Joao del Rei (UFSJ), Sao Joao del Rei; [d] Instituto de Fisica, Universidade de Sao Paulo, Sao Paulo, Brazil

25 Physics Department, Brookhaven National Laboratory, Upton NY, United States of America

26 [a] Transilvania University of Brasov, Brasov, Romania; [b] National Institute of Physics and Nuclear Engineering, Bucharest; [c] National Institute for Research and Development of Isotopic and Molecular Technologies, Physics Department, Cluj Napoca; [d] University Politehnica Bucharest, Bucharest; [e] West University in Timisoara, Timisoara, Romania

27 Departamento de Física, Universidad de Buenos Aires, Buenos Aires, Argentina

28 Cavendish Laboratory, University of Cambridge, Cambridge, United Kingdom

29 Department of Physics, Carleton University, Ottawa ON, Canada

30 CERN, Geneva, Switzerland

31 Enrico Fermi Institute, University of Chicago, Chicago IL, United States of America

32 [a] Departamento de Física, Pontificia Universidad Católica de Chile, Santiago; [b] Departamento de Física, Universidad Técnica Federico Santa María, Valparaíso, Chile

33 [a] Institute of High Energy Physics, Chinese Academy of Sciences, Beijing; [b] Department of Modern Physics, University of Science and Technology of China, Anhui; [c] Department of Physics, Nanjing University, Jiangsu; [d] School of Physics, Shandong University, Shandong; [e] Department of Physics and Astronomy, Shanghai Key Laboratory for Particle Physics and Cosmology, Shanghai Jiao Tong University, Shanghai; [f] Physics Department, Tsinghua University, Beijing 100084, China

34 Laboratoire de Physique Corpusculaire, Clermont Université and Université Blaise Pascal and CNRS/IN2P3, Clermont-Ferrand, France

35 Nevis Laboratory, Columbia University, Irvington NY, United States of America

36 Niels Bohr Institute, University of Copenhagen, Kobenhavn, Denmark

37 [a] INFN Gruppo Collegato di Cosenza, Laboratori Nazionali di Frascati; [b] Dipartimento di Fisica, Università della Calabria, Rende, Italy

38 [a] AGH University of Science and Technology, Faculty of Physics and Applied Computer Science, Krakow; [b] Marian Smoluchowski Institute of Physics, Jagiellonian University, Krakow, Poland

39 Institute of Nuclear Physics Polish Academy of Sciences, Krakow, Poland

40 Physics Department, Southern Methodist University, Dallas TX, United States of America

41 Physics Department, University of Texas at Dallas, Richardson TX, United States of America

42 DESY, Hamburg and Zeuthen, Germany

43 Institut für Experimentelle Physik IV, Technische Universität Dortmund, Dortmund, Germany

44 Institut für Kern- und Teilchenphysik, Technische Universität Dresden, Dresden, Germany

45 Department of Physics, Duke University, Durham NC, United States of America

46 SUPA - School of Physics and Astronomy, University of Edinburgh, Edinburgh, United Kingdom

47 INFN Laboratori Nazionali di Frascati, Frascati, Italy

48 Fakultät für Mathematik und Physik, Albert-Ludwigs-Universität, Freiburg, Germany

49 Section de Physique, Université de Genève, Geneva, Switzerland

50 [a] INFN Sezione di Genova; [b] Dipartimento di Fisica, Università di Genova, Genova, Italy

51 (a) E. Andronikashvili Institute of Physics, Iv. Javakhishvili Tbilisi State University, Tbilisi; (b) High Energy Physics Institute, Tbilisi State University, Tbilisi, Georgia

52 II Physikalisches Institut, Justus-Liebig-Universität Giessen, Giessen, Germany

53 SUPA - School of Physics and Astronomy, University of Glasgow, Glasgow, United Kingdom

54 II Physikalisches Institut, Georg-August-Universität, Göttingen, Germany

55 Laboratoire de Physique Subatomique et de Cosmologie, Université Grenoble-Alpes, CNRS/IN2P3, Grenoble, France

56 Department of Physics, Hampton University, Hampton VA, United States of America

57 Laboratory for Particle Physics and Cosmology, Harvard University, Cambridge MA, United States of America

58 (a) Kirchhoff-Institut für Physik, Ruprecht-Karls-Universität Heidelberg, Heidelberg; (b) Physikalisches Institut, Ruprecht-Karls-Universität Heidelberg, Heidelberg; (c) ZITI Institut für technische Informatik, Ruprecht-Karls-Universität Heidelberg, Mannheim, Germany

59 Faculty of Applied Information Science, Hiroshima Institute of Technology, Hiroshima, Japan

60 (a) Department of Physics, The Chinese University of Hong Kong, Shatin, N.T., Hong Kong; (b) Department of Physics, The University of Hong Kong, Hong Kong; (c) Department of Physics, The Hong Kong University of Science and Technology, Clear Water Bay, Kowloon, Hong Kong, China

61 Department of Physics, Indiana University, Bloomington IN, United States of America

62 Institut für Astro- und Teilchenphysik, Leopold-Franzens-Universität, Innsbruck, Austria

63 University of Iowa, Iowa City IA, United States of America

64 Department of Physics and Astronomy, Iowa State University, Ames IA, United States of America

65 Joint Institute for Nuclear Research, JINR Dubna, Dubna, Russia

66 KEK, High Energy Accelerator Research Organization, Tsukuba, Japan

67 Graduate School of Science, Kobe University, Kobe, Japan

68 Faculty of Science, Kyoto University, Kyoto, Japan

69 Kyoto University of Education, Kyoto, Japan

70 Department of Physics, Kyushu University, Fukuoka, Japan

71 Instituto de Física La Plata, Universidad Nacional de La Plata and CONICET, La Plata, Argentina

72 Physics Department, Lancaster University, Lancaster, United Kingdom

73 (a) INFN Sezione di Lecce; (b) Dipartimento di Matematica e Fisica, Università del Salento, Lecce, Italy

74 Oliver Lodge Laboratory, University of Liverpool, Liverpool, United Kingdom

75 Department of Physics, Jožef Stefan Institute and University of Ljubljana, Ljubljana, Slovenia

76 School of Physics and Astronomy, Queen Mary University of London, London, United Kingdom

77 Department of Physics, Royal Holloway University of London, Surrey, United Kingdom

78 Department of Physics and Astronomy, University College London, London, United Kingdom

79 Louisiana Tech University, Ruston LA, United States of America

80 Laboratoire de Physique Nucléaire et de Hautes Energies, UPMC and Université Paris-Diderot and CNRS/IN2P3, Paris, France

81 Fysiska institutionen, Lunds universitet, Lund, Sweden

82 Departamento de Fisica Teorica C-15, Universidad Autonoma de Madrid, Madrid, Spain

83 Institut für Physik, Universität Mainz, Mainz, Germany

84 School of Physics and Astronomy, University of Manchester, Manchester, United Kingdom

85 CPPM, Aix-Marseille Université and CNRS/IN2P3, Marseille, France

86 Department of Physics, University of Massachusetts, Amherst MA, United States of America

87 Department of Physics, McGill University, Montreal QC, Canada

88 School of Physics, University of Melbourne, Victoria, Australia

89 Department of Physics, The University of Michigan, Ann Arbor MI, United States of America

90 Department of Physics and Astronomy, Michigan State University, East Lansing MI, United States of America

91 (a) INFN Sezione di Milano; (b) Dipartimento di Fisica, Università di Milano, Milano, Italy

92 B.I. Stepanov Institute of Physics, National Academy of Sciences of Belarus, Minsk, Republic of Belarus

[93] National Scientific and Educational Centre for Particle and High Energy Physics, Minsk, Republic of Belarus

[94] Department of Physics, Massachusetts Institute of Technology, Cambridge MA, United States of America

[95] Group of Particle Physics, University of Montreal, Montreal QC, Canada

[96] P.N. Lebedev Institute of Physics, Academy of Sciences, Moscow, Russia

[97] Institute for Theoretical and Experimental Physics (ITEP), Moscow, Russia

[98] National Research Nuclear University MEPhI, Moscow, Russia

[99] D.V. Skobeltsyn Institute of Nuclear Physics, M.V. Lomonosov Moscow State University, Moscow, Russia

[100] Fakultät für Physik, Ludwig-Maximilians-Universität München, München, Germany

[101] Max-Planck-Institut für Physik (Werner-Heisenberg-Institut), München, Germany

[102] Nagasaki Institute of Applied Science, Nagasaki, Japan

[103] Graduate School of Science and Kobayashi-Maskawa Institute, Nagoya University, Nagoya, Japan

[104] [a] INFN Sezione di Napoli; [b] Dipartimento di Fisica, Università di Napoli, Napoli, Italy

[105] Department of Physics and Astronomy, University of New Mexico, Albuquerque NM, United States of America

[106] Institute for Mathematics, Astrophysics and Particle Physics, Radboud University Nijmegen/Nikhef, Nijmegen, Netherlands

[107] Nikhef National Institute for Subatomic Physics and University of Amsterdam, Amsterdam, Netherlands

[108] Department of Physics, Northern Illinois University, DeKalb IL, United States of America

[109] Budker Institute of Nuclear Physics, SB RAS, Novosibirsk, Russia

[110] Department of Physics, New York University, New York NY, United States of America

[111] Ohio State University, Columbus OH, United States of America

[112] Faculty of Science, Okayama University, Okayama, Japan

[113] Homer L. Dodge Department of Physics and Astronomy, University of Oklahoma, Norman OK, United States of America

[114] Department of Physics, Oklahoma State University, Stillwater OK, United States of America

[115] Palacký University, RCPTM, Olomouc, Czech Republic

[116] Center for High Energy Physics, University of Oregon, Eugene OR, United States of America

[117] LAL, Université Paris-Sud and CNRS/IN2P3, Orsay, France

[118] Graduate School of Science, Osaka University, Osaka, Japan

[119] Department of Physics, University of Oslo, Oslo, Norway

[120] Department of Physics, Oxford University, Oxford, United Kingdom

[121] [a] INFN Sezione di Pavia; [b] Dipartimento di Fisica, Università di Pavia, Pavia, Italy

[122] Department of Physics, University of Pennsylvania, Philadelphia PA, United States of America

[123] National Research Centre "Kurchatov Institute" B.P.Konstantinov Petersburg Nuclear Physics Institute, St. Petersburg, Russia

[124] [a] INFN Sezione di Pisa; [b] Dipartimento di Fisica E. Fermi, Università di Pisa, Pisa, Italy

[125] Department of Physics and Astronomy, University of Pittsburgh, Pittsburgh PA, United States of America

[126] [a] Laboratório de Instrumentação e Física Experimental de Partículas - LIP, Lisboa; [b] Faculdade de Ciências, Universidade de Lisboa, Lisboa; [c] Department of Physics, University of Coimbra, Coimbra; [d] Centro de Física Nuclear da Universidade de Lisboa, Lisboa; [e] Departamento de Fisica, Universidade do Minho, Braga; [f] Departamento de Fisica Teorica y del Cosmos and CAFPE, Universidad de Granada, Granada (Spain); [g] Dep Fisica and CEFITEC of Faculdade de Ciencias e Tecnologia, Universidade Nova de Lisboa, Caparica, Portugal

[127] Institute of Physics, Academy of Sciences of the Czech Republic, Praha, Czech Republic

[128] Czech Technical University in Prague, Praha, Czech Republic

[129] Faculty of Mathematics and Physics, Charles University in Prague, Praha, Czech Republic

[130] State Research Center Institute for High Energy Physics (Protvino), NRC KI,Russia, Russia

131 Particle Physics Department, Rutherford Appleton Laboratory, Didcot, United Kingdom

132 [a] INFN Sezione di Roma; [b] Dipartimento di Fisica, Sapienza Università di Roma, Roma, Italy

133 [a] INFN Sezione di Roma Tor Vergata; [b] Dipartimento di Fisica, Università di Roma Tor Vergata, Roma, Italy

134 [a] INFN Sezione di Roma Tre; [b] Dipartimento di Matematica e Fisica, Università Roma Tre, Roma, Italy

135 [a] Faculté des Sciences Ain Chock, Réseau Universitaire de Physique des Hautes Energies - Université Hassan II, Casablanca; [b] Centre National de l'Energie des Sciences Techniques Nucleaires, Rabat; [c] Faculté des Sciences Semlalia, Université Cadi Ayyad, LPHEA-Marrakech; [d] Faculté des Sciences, Université Mohamed Premier and LPTPM, Oujda; [e] Faculté des sciences, Université Mohammed V, Rabat, Morocco

136 DSM/IRFU (Institut de Recherches sur les Lois Fondamentales de l'Univers), CEA Saclay (Commissariat à l'Energie Atomique et aux Energies Alternatives), Gif-sur-Yvette, France

137 Santa Cruz Institute for Particle Physics, University of California Santa Cruz, Santa Cruz CA, United States of America

138 Department of Physics, University of Washington, Seattle WA, United States of America

139 Department of Physics and Astronomy, University of Sheffield, Sheffield, United Kingdom

140 Department of Physics, Shinshu University, Nagano, Japan

141 Fachbereich Physik, Universität Siegen, Siegen, Germany

142 Department of Physics, Simon Fraser University, Burnaby BC, Canada

143 SLAC National Accelerator Laboratory, Stanford CA, United States of America

144 [a] Faculty of Mathematics, Physics & Informatics, Comenius University, Bratislava; [b] Department of Subnuclear Physics, Institute of Experimental Physics of the Slovak Academy of Sciences, Kosice, Slovak Republic

145 [a] Department of Physics, University of Cape Town, Cape Town; [b] Department of Physics, University of Johannesburg, Johannesburg; [c] School of Physics, University of the Witwatersrand, Johannesburg, South Africa

146 [a] Department of Physics, Stockholm University; [b] The Oskar Klein Centre, Stockholm, Sweden

147 Physics Department, Royal Institute of Technology, Stockholm, Sweden

148 Departments of Physics & Astronomy and Chemistry, Stony Brook University, Stony Brook NY, United States of America

149 Department of Physics and Astronomy, University of Sussex, Brighton, United Kingdom

150 School of Physics, University of Sydney, Sydney, Australia

151 Institute of Physics, Academia Sinica, Taipei, Taiwan

152 Department of Physics, Technion: Israel Institute of Technology, Haifa, Israel

153 Raymond and Beverly Sackler School of Physics and Astronomy, Tel Aviv University, Tel Aviv, Israel

154 Department of Physics, Aristotle University of Thessaloniki, Thessaloniki, Greece

155 International Center for Elementary Particle Physics and Department of Physics, The University of Tokyo, Tokyo, Japan

156 Graduate School of Science and Technology, Tokyo Metropolitan University, Tokyo, Japan

157 Department of Physics, Tokyo Institute of Technology, Tokyo, Japan

158 Department of Physics, University of Toronto, Toronto ON, Canada

159 [a] TRIUMF, Vancouver BC; [b] Department of Physics and Astronomy, York University, Toronto ON, Canada

160 Faculty of Pure and Applied Sciences, and Center for Integrated Research in Fundamental Science and Engineering, University of Tsukuba, Tsukuba, Japan

161 Department of Physics and Astronomy, Tufts University, Medford MA, United States of America

162 Centro de Investigaciones, Universidad Antonio Narino, Bogota, Colombia

163 Department of Physics and Astronomy, University of California Irvine, Irvine CA, United States of America

164 [a] INFN Gruppo Collegato di Udine, Sezione di Trieste, Udine; [b] ICTP, Trieste; [c] Dipartimento di Chimica, Fisica e Ambiente, Università di Udine, Udine, Italy

[165] Department of Physics, University of Illinois, Urbana IL, United States of America

[166] Department of Physics and Astronomy, University of Uppsala, Uppsala, Sweden

[167] Instituto de Física Corpuscular (IFIC) and Departamento de Física Atómica, Molecular y Nuclear and Departamento de Ingeniería Electrónica and Instituto de Microelectrónica de Barcelona (IMB-CNM), University of Valencia and CSIC, Valencia, Spain

[168] Department of Physics, University of British Columbia, Vancouver BC, Canada

[169] Department of Physics and Astronomy, University of Victoria, Victoria BC, Canada

[170] Department of Physics, University of Warwick, Coventry, United Kingdom

[171] Waseda University, Tokyo, Japan

[172] Department of Particle Physics, The Weizmann Institute of Science, Rehovot, Israel

[173] Department of Physics, University of Wisconsin, Madison WI, United States of America

[174] Fakultät für Physik und Astronomie, Julius-Maximilians-Universität, Würzburg, Germany

[175] Fachbereich C Physik, Bergische Universität Wuppertal, Wuppertal, Germany

[176] Department of Physics, Yale University, New Haven CT, United States of America

[177] Yerevan Physics Institute, Yerevan, Armenia

[178] Centre de Calcul de l'Institut National de Physique Nucléaire et de Physique des Particules (IN2P3), Villeurbanne, France

[a] Also at Department of Physics, King's College London, London, United Kingdom

[b] Also at Institute of Physics, Azerbaijan Academy of Sciences, Baku, Azerbaijan

[c] Also at Novosibirsk State University, Novosibirsk, Russia

[d] Also at TRIUMF, Vancouver BC, Canada

[e] Also at Department of Physics & Astronomy, University of Louisville, Louisville, KY, United States of America

[f] Also at Department of Physics, California State University, Fresno CA, United States of America

[g] Also at Department of Physics, University of Fribourg, Fribourg, Switzerland

[h] Also at Departamento de Fisica e Astronomia, Faculdade de Ciencias, Universidade do Porto, Portugal

[i] Also at Tomsk State University, Tomsk, Russia

[j] Also at CPPM, Aix-Marseille Université and CNRS/IN2P3, Marseille, France

[k] Also at Universita di Napoli Parthenope, Napoli, Italy

[l] Also at Institute of Particle Physics (IPP), Canada

[m] Also at Particle Physics Department, Rutherford Appleton Laboratory, Didcot, United Kingdom

[n] Also at Department of Physics, St. Petersburg State Polytechnical University, St. Petersburg, Russia

[o] Also at Department of Physics, The University of Michigan, Ann Arbor MI, United States of America

[p] Also at Louisiana Tech University, Ruston LA, United States of America

[q] Also at Institucio Catalana de Recerca i Estudis Avancats, ICREA, Barcelona, Spain

[r] Also at Graduate School of Science, Osaka University, Osaka, Japan

[s] Also at Department of Physics, National Tsing Hua University, Taiwan

[t] Also at Department of Physics, The University of Texas at Austin, Austin TX, United States of America

[u] Also at Institute of Theoretical Physics, Ilia State University, Tbilisi, Georgia

[v] Also at CERN, Geneva, Switzerland

[w] Also at Georgian Technical University (GTU),Tbilisi, Georgia

[x] Also at Manhattan College, New York NY, United States of America

[y] Also at Hellenic Open University, Patras, Greece

[z] Also at Institute of Physics, Academia Sinica, Taipei, Taiwan

[aa] Also at LAL, Université Paris-Sud and CNRS/IN2P3, Orsay, France

[ab] Also at Academia Sinica Grid Computing, Institute of Physics, Academia Sinica, Taipei, Taiwan

[ac] Also at School of Physics, Shandong University, Shandong, China

[ad] Also at Moscow Institute of Physics and Technology State University, Dolgoprudny, Russia

[ae] Also at Section de Physique, Université de Genève, Geneva, Switzerland

[af] Also at International School for Advanced Studies (SISSA), Trieste, Italy

[ag] Also at Department of Physics and Astronomy, University of South Carolina, Columbia SC, United States of America

[ah] Also at School of Physics and Engineering, Sun Yat-sen University, Guangzhou, China

[ai] Also at Faculty of Physics, M.V.Lomonosov Moscow State University, Moscow, Russia

[aj] Also at National Research Nuclear University MEPhI, Moscow, Russia

[ak] Also at Department of Physics, Stanford University, Stanford CA, United States of America

[al] Also at Institute for Particle and Nuclear Physics, Wigner Research Centre for Physics, Budapest, Hungary

[am] Also at University of Malaya, Department of Physics, Kuala Lumpur, Malaysia

[*] Deceased